Final Report

for

Latching Ferrite Switch

(May 1967 - June 1968)

Contract No.: NAS5-10422

Goddard Space Flight Center

Contracting Officer: Gary B. Burkholder
Technical Monitor: Milton K. Mills 731

Prepared by:

Scientific-Atlanta, Inc.
P. O. Box 13654
Atlanta, Georgia 30324

for

Goddard Space Flight Center
Greenbelt, Maryland

Final Report

for

Latching Ferrite Switch

(May 1967 - June 1968)

Contract No.: NAS5-10422

Prepared by

Scientific-Atlanta, Inc.
P. O. Box 13654
Atlanta, Georgia 30324

for

Goddard Space Flight Center
Greenbelt, Maryland

Final Report

for

Latching Ferrite Switch

(May 1967 - June 1968)

Contract No.: NAS5-10422

Goddard Space Flight Center

Contracting Officer: Gary B. Burkholder
Technical Monitor: Milton K. Mills

Prepared by:

Scientific-Atlanta, Inc.
P. O. Box 13654
Atlanta, Georgia 30324

for

Goddard Space Flight Center
Greenbelt, Maryland

TABLE OF CONTENTS

LIST OF ILLUSTRATIONS

LIST OF ILLUSTRATIONS - Continued

LIST OF TABLES

1. ABSTRACT

1.1 Program Requirements

Scientific-Atlanta, Inc. submits this final report on Contract NAS5-10422 to NASA/GSFC. Under this contract, Scientific-Atlanta, Inc. designed and constructed a latching ferrite SP16T switch and combiner network per RFP733-47644, the specifications of which are reproduced verbatim below:

"A. Electrical Specifications:

(a) Switch Type: Indicated in Figure 1

(b) Frequency: 7.9 to 8.1 GHz for circulators 1 through 15; 7.2 to 8.1 GHz for all other circulators.

(c) Insertion Loss: 0.3 dB maximum/switch section for circulators 1 through 15; 0.4 dB maximum/switch section for all other circulators.

(d) Isolation: 20 dB minimum with design goal of 25 dB
(e) Power Handling Capability: 30 watts average
(f) Switching Time: 20 μsec
(g) Switching Rate: 1 KHz maximum
(h) Total Switching Energy/pole required from power supply: 2500/mJ max.
(i) Driver Supply Voltage: 28 vdc at 2% regulation
(j) Trigger Pulse Required: 10 v nominal into 50 ohms for trigger pulse rise time faster than 1 μsec (a separate input pulse for each sw state).
(k) D.C. Blocks: Must suppress switching transients from latching circulators.
(l) Insertion Phase: The insertion phase between all wideband circulators (7.2 to 8.1 GHz) must be not greater than ±5 degrees between units from -20°F to 125°F. The insertion phase between units located in monopulse comparator must be not greater than ±1 degree at room temperature.
(m) RF connectors: Type N
(n) Nominal Impedance: 50 ohms
(o) VSWR: Not greater than 1.25:1
(p) Monopulse Characteristics:
1. Insertion Loss: The insertion loss shall be not greater than 1 db from the input terminals to Δ Az, Δ EL, or Σ outputs.
2. Isolation: The isolation shall be equal to or greater than 20 dB between monopulse output terminals.
3. VSWR: The VSWR of each monopulse terminal shall not exceed 1.25:1.
(q) Trigger Pulse Generator Characteristics:
1. Function: A control box with necessary logic shall be supplied to generate required trigger pulses to select at the output terminal the sum of terminals 1 and 2 or the sum of terminals 2 and 3.... sum of terminals 15 and A & B, or

monopulse operation. Sixteen control switches will be required (no two adjacent switches will be required to be energized.)

2. All trigger pulse characteristics must be compatible with the requirements.

3. Power Requirements: 28 vdc of paragraph 1 A (j)

4. Size: 1 ft. x 0.5 ft. x 0.5 ft. maximum

B. Mechanical Characteristics:

(a) Size: 13 in. x 10 in. x 5 in. maximum
(b) Configuration: See Figure 2
(c) Weight: To be supplied by contractor"

1.2 Program Accomplishment

A ferrite latching switch and combiner was constructed meeting virtually all of the detailed specifications.

A basic latching circulator was designed which had a typical insertion loss of 0.2 dB, and an isolation exceeding 20 dB over the temperature extremes. The limits of switching speed and the switching energy of this device were very close to the specified requirements. Because this was a prototype primarily used to evaluate a system concept, no effort was devoted to integrating the microwave components. As a result rigid coax was used to interconnect the 33 latching circulators. The total switch insertion loss was about 2.5 dB, of which about half of this was directly contributed by the cable. Aside from this, the switch functioned as predicted giving excellent isolation between undesired channels and worked well over the required temperature extremes.

It is recommended that future switches of this type be designed as microwave integrated circuits in order to minimize insertion loss.

2. TECHNICAL BACKGROUND: STRIPLINE LATCHING CIRCULATORS

2.1 Introduction

Y-junction circulators have been known for a long time, and a great amount of work has recently gone into the development of suitable structures for broad-banding these devices.[1] However, the requirement herein that the proposed devices be of the latching variety, and that they achieve fast switching with very low energy electrical pulses demands new design techniques.

To satisfy the switching and latching requirements, it is clear that ferrites with closed magnetic paths must be employed, and that these ferrites must have both good square loop properties and good microwave properties (for that part of the ferrite in the microwave field). These ferrites must be utilized in appropriate configurations, similar to those which have already been studied for more conventional permanent magnet circulators. Switching is accomplished by reversing the direction of magnetization.

Most of the true latching devices investigated prior to Scientific-Atlanta's work in latching circulators (e.g., latching phase shifters, latching waveguide circulators, etc.) utilized ferrite toroids which were fabricated in one piece and contained entirely within the waveguide or transmission line structure. In early development work in this laboratory, consideration was given to the possibility of constructing a stripline latching circulator in this manner, i.e., with two ferrite toroids, one above and one below the center conductor, both of which would be wholly within the region of microwave interaction. Such a device, if it were practically realizable, would require very low switching energy and exhibit great switching speed. However, previous experience, both here and elsewhere, indicates that such an approach does not produce practical devices in stripline. This seems to be due to the fact that TEM circulators require ferrite elements with relatively large dimensions measured in a plane parallel to the ground planes, as compared to the small ground plane spacing dictated by the necessity of suppressing higher order modes. This unfavorable aspect ratio makes it impossible to hold the center portion of the toroid at a satisfactorily high remanent state. For this reason, it has been necessary to construct latching TEM circulators with the required magnetic return path provided outside the microwave structure, and shielded from the RF energy. Devices of this type are called "external return path" circulators, and will be discussed in greater detail later in this section.

2.2 Three-Port Junction Circulator Theory

While most of the previous development work on junction circulators was accomplished without benefit of an established theoretical approach, some recent work by Bosma[2,3], and Fay and Comstock[4,5] give useful design equations for stripline circulators and provide information which relates bandwidth and the properties of ferrimagnetic materials. Although this theory was developed for circulators having an applied magnetic field, it will also provide guidance for building latching circulators. A brief summary of the results of the theory is given here, as extracted from the Final Report under Contract No. DA36-039SC-89214. The major portion of Bosma's design equations deals primarily with above-resonance circulator operation while the work done by Fay and Comstock is slanted to below-resonance operation. Because the interest here is in latching devices, the below-resonance case will be discussed.

The ferrite geometry treated by Fay and Comstock is as shown in Figure 1. The propagation constant, Γ, is defined as

$$\Gamma^2 = \omega^2 \epsilon \, \epsilon_o \mu_{eff} \mu_o \tag{1}$$

where

$$\mu_{eff} = \frac{\mu^2 - \kappa^2}{\mu} \tag{2}$$

and μ and κ are the usual components of the Polder tensor.

The solution of the boundary value problem provided an equation for the ferrite radius which was given by

$$R = \frac{1.84\lambda}{2\pi\sqrt{\mu_{eff}\,\epsilon_r}} \tag{3}$$

where μ_{eff} is as shown in Figure 2.

The input wave admittance, Y_w, of the ferrite disk is

$$Y_w = \frac{Y_{eff}\left|\kappa/\mu\right|}{\sin\psi} \tag{4}$$

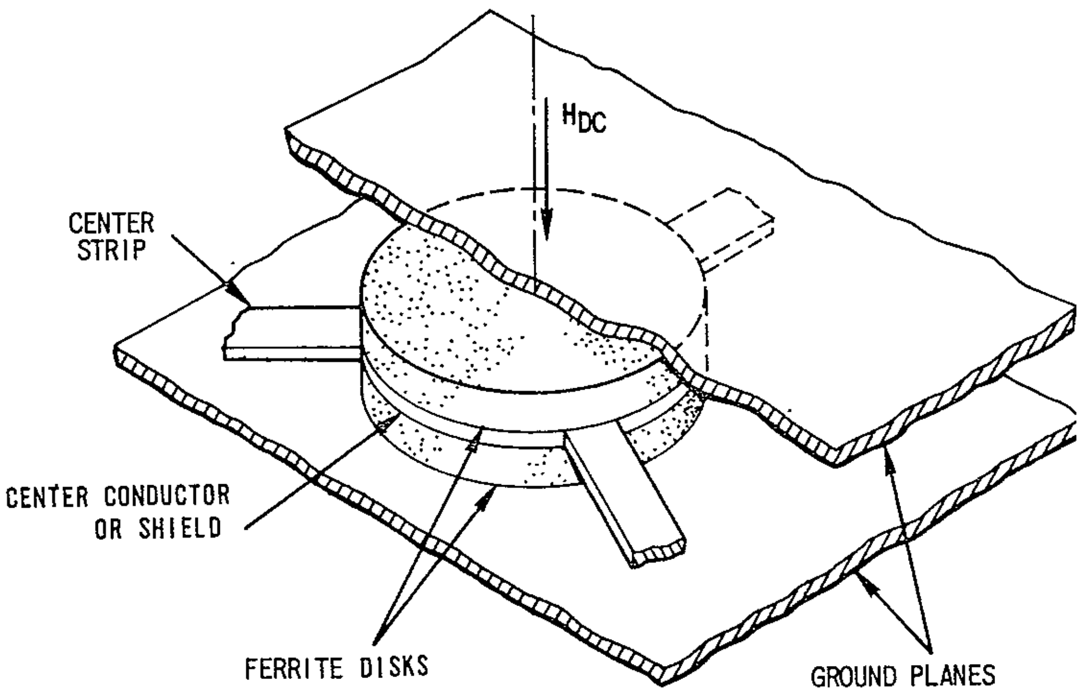

Figure 1. Strip Transmission Line Y-Junction Circulator
(after Fay & Comstock)

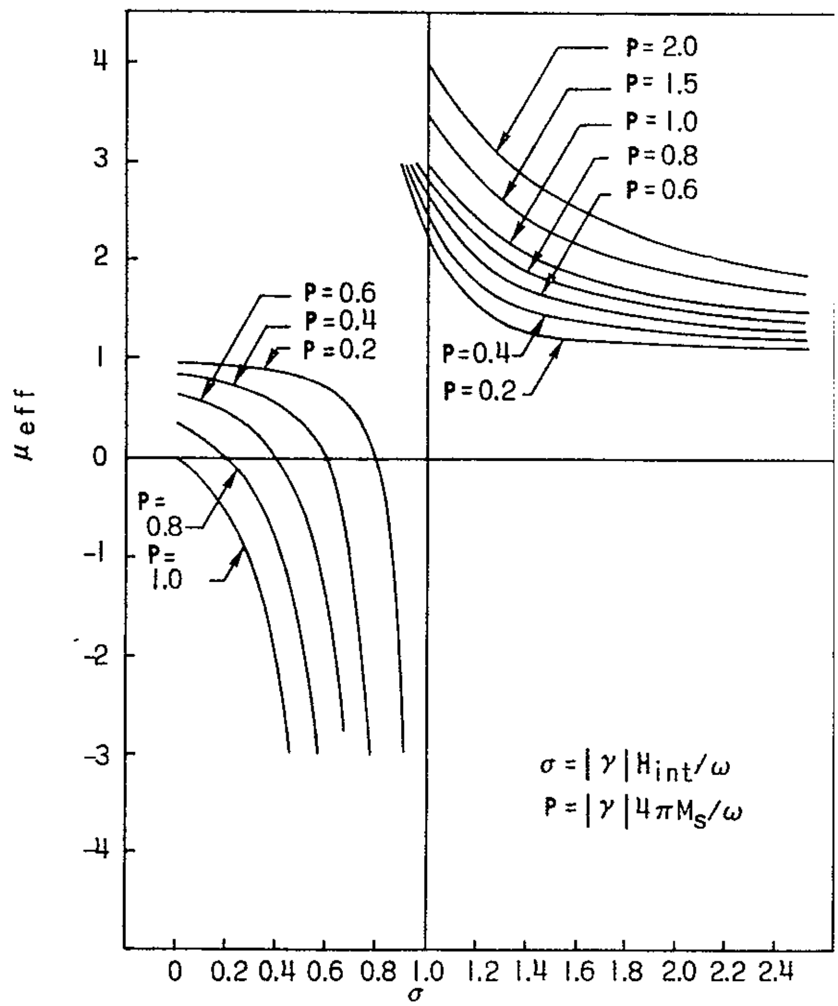

Figure 2. μ_{eff} Versus σ for Ferrite Circulators (after Fay & Comstock)

where

$$Y_{eff} = \sqrt{\frac{\epsilon \epsilon_o}{\mu_o \mu_{eff}}} \qquad (5)$$

and ψ is defined in Figure 3.

The loaded Q, Q_L, of the circulator was found to be

$$Q_L = \frac{1.48 \omega R^2 \epsilon \epsilon_o}{Y_w d} \qquad (6)$$

where d is the disk thickness. If a quarter-wave transformer is used for matching the ferrite resonator, as in the case here, a Q can be derived which relates bandwidth 2δ and the desired maximum VSWR.

This is given by

$$Q_L = \frac{\tan \theta}{2\delta} \qquad (7)$$

where

$$\theta = \sec^{-1}\sqrt{VSWR_{max}} \qquad (8)$$

The ferrite parameters can be related to Q_L by the approximate relation

$$\kappa/\mu \approx \frac{0.71}{Q_L} \qquad (9)$$

The value of the constant in the above equation is approximately correct for values of κ/μ in the 0.25 to 0.5 range, which will cover most of the practical cases.

These equations are generally utilized in reverse to their presentation since the isolation bandwidth of the circulator is generally specified. This isolation usually corresponds quite closely to the return loss at the input port, and the return loss at this port can be converted to VSWR. Using this information and the desired bandwidth, the value of κ/μ can be computed.

For minimum field requirements it is convenient to operate at $H_{dc} \approx N_z 4\pi M_s$ (just saturated) or $\sigma = 0$ (see Figure 2). From Figures 2 and 4 it can be seen that at $\sigma = 0$, $(\kappa/\mu) = P$, and $\mu_{eff} = 1 - (\kappa/\mu)^2$.

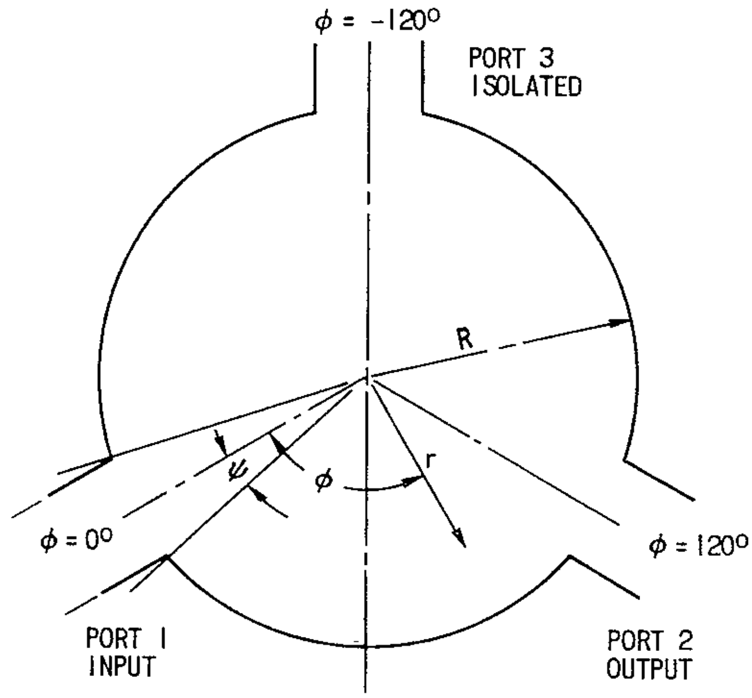

Figure 3. Center Conductor Geometry (after Bosma)

It has been found experimentally that for values of σ slightly greater than zero, resonance losses become apparent at the lower frequencies. For values of σ considerably less than 0, the bandwidth becomes limited. Thus, the value $\sigma = 0$ is a realistic number to choose for fixed circulator design, and applies approximately for latching devices. Using this value of σ and the computed value of κ/μ, μ_{eff} can be computed (or obtained from Figure 2). It is now possible to calculate the ferrite disk radius from equation (3). It also can be deduced from the curves of Figure 4 that the bandwidth will vary rapidly with $4\pi M$ in the below-resonance region ($\sigma < 1$). This has also been shown to be true experimentally. Thus it would appear desirable in the latching circulator to maintain a constant remanent value of $4\pi M$, to maintain bandwidth.

While this theoretical approach provides considerable insight into the operation of the circulator, it must be pointed out that, due to the complexity of the problem, it is impossible to specify all of the parameters with sufficient accuracy to actually produce a "paper design." The above design criteria do not include information on various loss mechanisms (dielectric and magnetic) and their relationships to the values of H_a, $4\pi M_s$, ΔH, ϵ, ϵ'', μ'', etc. which are encountered in practical applications.

In addition to the theoretical contributions outlined above, considerable empirical effort has been directed toward the design of broadband stripline junction circulators. It was found that there are optimum values of ferrite puck diameter and saturation moment for obtaining maximum bandwidth. These values are graphically illustrated in Figure 5 where for 8.0 GHz the optimum diameter is around 0.300 inch and the saturation magnetization should be between 1400 and 2500 gauss.

It should be emphasized, however, that junction parameters discussed above are optimum only if broadband performance is required. As is well-known, any lossless, three-port, nonreciprocal, symmetrical junction will act as a circulator when the diagonal components of its scattering matrix are made equal to zero (i.e., when each of the three ports are matched). Thus these parameters are found to be optimum since they produce a device which may be matched over a wide range of frequencies. In the proposed system of interest here, none of the circulators are required to operate over an extremely wide range of frequencies, and hence, the junction configuration used may deviate somewhat from those values

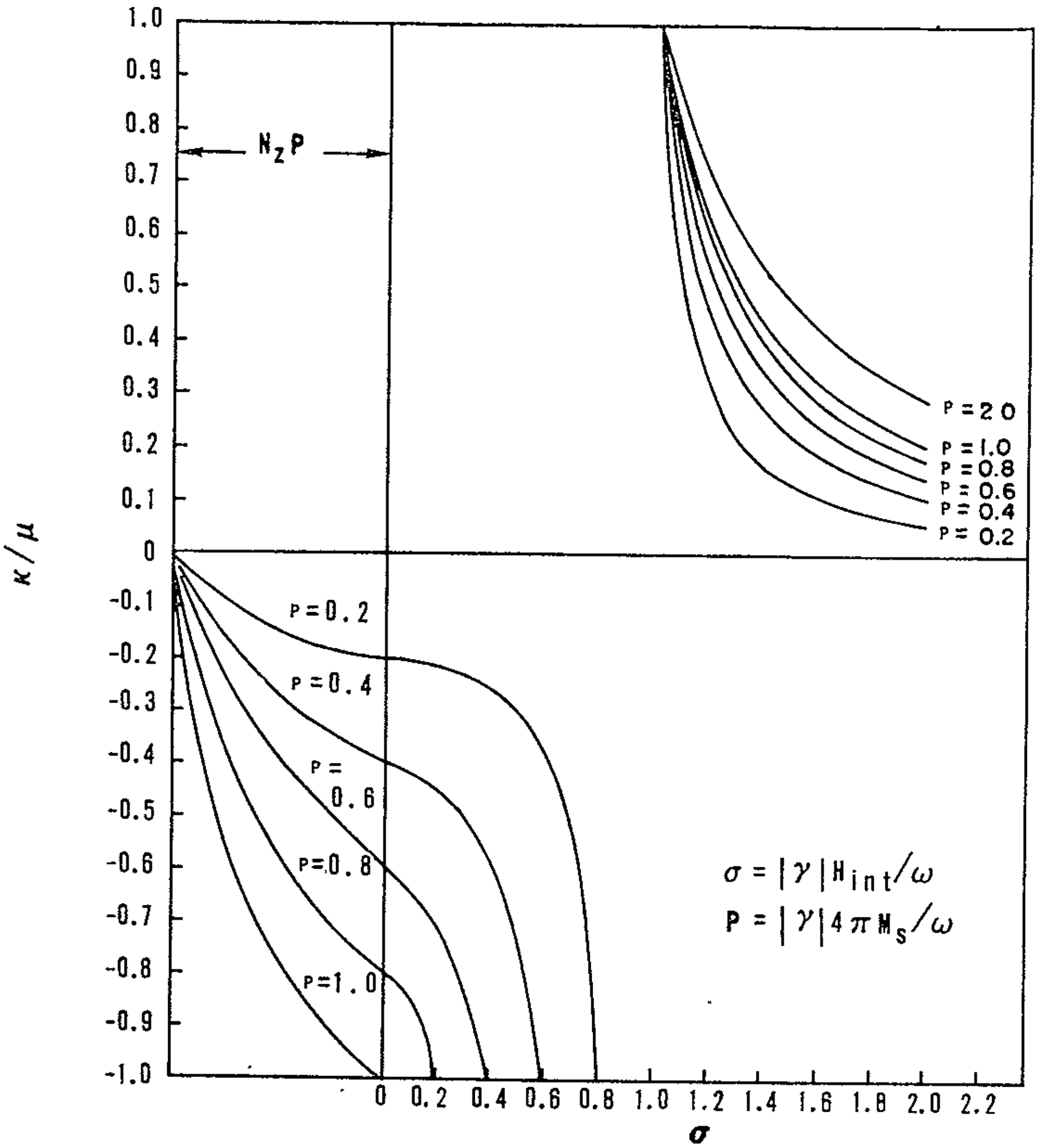

Figure 4. $\varkappa/\mu$ Versus σ where $\sigma = \frac{\gamma \ H_{int}}{\omega}$ (after Fay and Comstock)

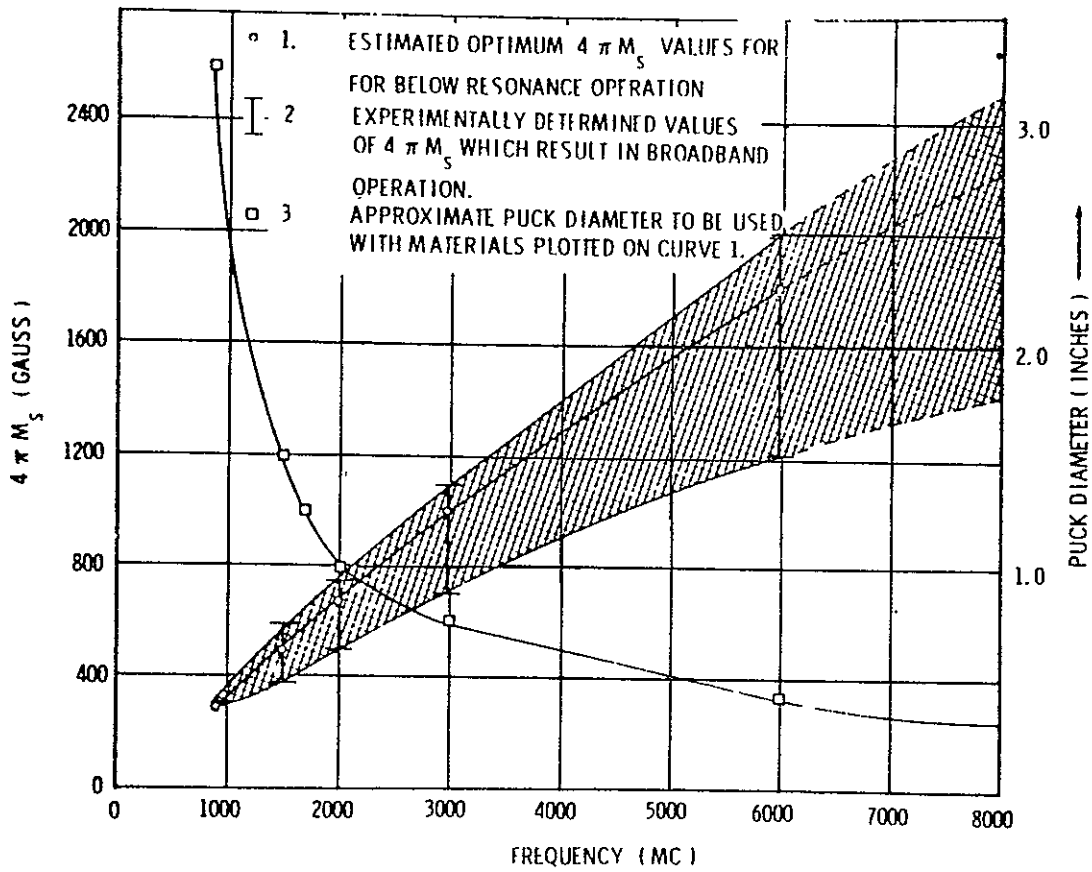

Figure 5. Envelope of Practical $4\pi M_s$ Values and Puck Diameters for Below-Resonance Broadband Operation

which are optimum for broadband operation. This would permit the reduction of switching energy by the use of a smaller volume of ferrite and, possibly, a material having a lower $4\pi M_s$.

2.3 Latching Circulator Configurations

Figures 6 and 7 illustrate the technique by which an essentially closed magnetic path is provided for the dc magnetization, while confining the RF energy to the microwave ferrite element. It is necessary that there be a conducting surface between the microwave ferrite element and the external return path in order to confine the microwave fields to the transmission line; in addition, the microwave center conductor must pass between the upper and lower ferrite elements. Thus, in this configuration, it is not possible to employ perfectly closed toroids as have been used in essentially all of the early developed latching microwave devices. Since the dc magnetic field passes through this conducting surface, eddy currents will be set up whenever the flux is reversed. Fortunately, however, the thickness of this conducting surface can be chosen to give satisfactory shielding and low insertion loss at microwave frequencies, and at the same time allow the reversal of the dc magnetization with little deterioration of the switching energy and time. This follows from the fact that the skin depth in a conducting material is inversely proportional to the square root of the frequency; thus, it is possible to make the waveguide wall thick, in terms of skin depths, at 8 GHz and thin, in terms of skin depths, at the highest frequency at which the magnetization will be reversed. The conducting sheet (ground plane or center conductor) will then appear to be infinitely thick to the microwave energy, but will suppress and quickly damp out eddy currents, assuring fast switching. It has been found experimentally that if these conducting surfaces are fabricated from thin (approximately 0.00025 inch) sheets of an appropriate metal, the device may be switched rapidly (in several microseconds) with no noticeable effect upon the microwave performance. Another noteworthy feature of the latching circulator housing is that the housing itself must not form a closed conducting path through the composite toroid, since the resulting shorted turn would tremendously increase switching time and energy.

The dimensions of the ferrite return path are chosen to produce the same magnetization found to be optimum when the junction is tested in a non-latching configuration. To some extent, this can be done theoretically by considering the

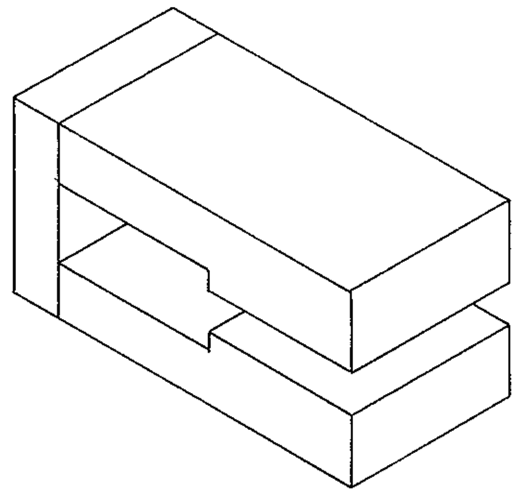

Figure 6. Return Path Configuration Used in Stripline Latching Circulator.

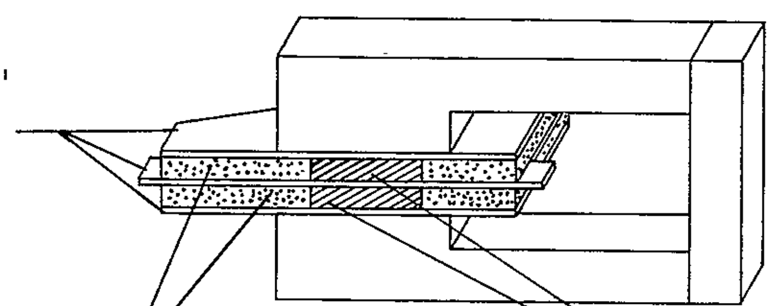

Figure 7. Illustration of Construction of Composite Magnetic Path in Stripline Latching Circulator.

length, cross-sectional area, and magnetic properties of both the ferrite element and return path, as well as the air gaps in the composite toroid. For final adjustments in the shape of the return path, it is necessary to actually observe the hysteresis loop of the composite toroid on a B-H loop plotter. The general design approach for the latching circulator was based on previous work by Stern and Ince[6] utilizing ferrite magnetic composite circuits. It has been found generally that broadband operation can be achieved when the ferrite circulator pucks are biased approximately to the saturation magnetization of the material. Composite circuits offer a particular advantage in that a remanence flux in the composite circuit can be attained which is equal to or greater than the intrinsic remanence flux of the microwave ferrite.

The general design shown in Figure 8 consists essentially of a driver-limiter ferrite located external to the microwave circuit. For the specific application here the yoke is not needed since the magnetization of the return path is close to that of the microwave material. The driver-limiter supplies the MMF necessary to sustain a remanent flux in the magnetic circuit and limits the flux supplied to the microwave ferrite. Limiting the flux is critical to temperature stabilization. The first restraint is that the driver MMF be equal to or greater than the MMF drops in the microwave ferrite and gaps between circuit elements such that the following equation is satisfied:

$$dH_d \geq mH_m + gH_g. \tag{10}$$

The terms d, m, and g are the mean flux path lengths of the driver, microwave element, and the accumulative air gaps of the circuit, and H_d, H_m, and H_g are the coercive force of the driver material, coercive force of the microwave material and the magnetic field intensity across the air gaps, respectively.

Secondly, the flux through the microwave ferrite is limited so that

$$DB_d \leq MB_m \tag{11}$$

where D and M are the cross-sectional areas of the driver-limiter and the microwave ferrite, and B_d and B_m refer to the maximum flux density of

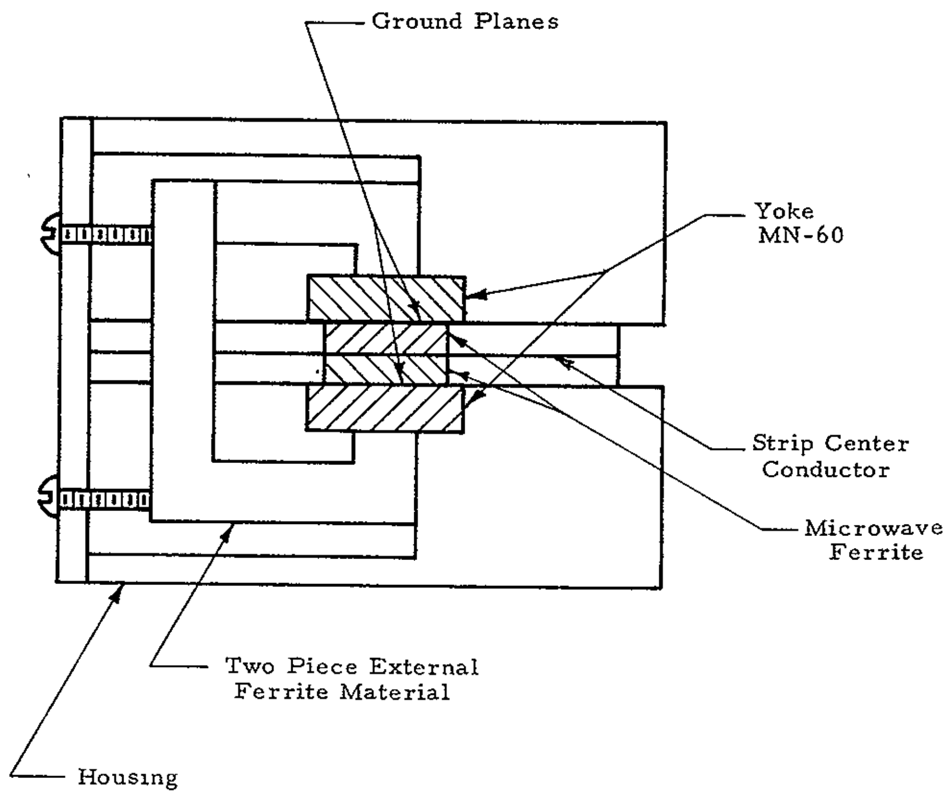

Figure 8. Typical Design of an External Return Path.

the driver-limiter and microwave element, respectively. The cross-section, D, for a practical circuit must be increased somewhat from the value given by equation (11) for flux leakage considerations.

From a practical consideration, an exact calculated design is very difficult to accomplish. Although most of the material parameters are known quite accurately, it is difficult to predict with accuracy the gap length or the flux lost through fringing. For example, the MMF drop across an air gap is calculated by estimating g of equation (10), which is on the order of 10^{-2} to 10^{-3} cm. and multiplying this by H_g, which is on the order of 10^3 . The estimate of g is complicated by the fact that there are often as many as five to seven gaps. Thus, it is felt that considerable experience is needed to estimate the values required in equation (10) with any degree of accuracy.

Another factor which is difficult to estimate and limits the accuracy of a calculated design is the leakage flux for a particular magnetic circuit. In general, the cross-section of the driver limiter must be increased to account for these losses. Although Stern and Ince provide helpful equations for estimating the leakage flux, it is, in fact, difficult to accomplish with accuracy in a complex arrangement such as is encountered in a latching circulator.

2.4 Switching Energy Considerations

The energy required in switching a latching device of this type may be divided into three categories:

(1) Energy lost in the electronic driver circuitry.
(2) Energy lost due to eddy currents in the ground planes and center conductor.
(3) Energy required to reverse the magnetization of the ferrite toroid (hysteresis loss).

Electronic driver loss will not be discussed at this time, but it has been demonstrated on several devices of this type that this energy need not represent more than about 25 % of the total, provided appropriate circuits are included in the driver to minimize this loss.

The energy consumed by eddy currents depends upon a number of factors (including the physical parameters of the composite toroid and the required switching time) and, as yet, has not been calculated analytically. As was mentioned previously, however, if the desired microwave frequency is as high as 8 GHz, the conducting surfaces may be made extremely thin and will present a high resistance to eddy currents. Experimental evidence indicates that (at this frequency) total eddy current losses would not exceed 40 or 50% of the total energy consumed.

The loss due to flux reversal in the composite toroid, on the other hand, may be approximately calculated. The energy required per cubic centimeter for switching at speeds as low as several microseconds is given by the equation

$$w = \frac{1}{4\pi} \int \vec{H} \cdot d\vec{B} , \qquad (12)$$

where the integral is carried half way around the hysteresis loop. For square loop ferrites this yields

$$W \approx 2M_sH_cV \times 10^{-7} \text{ joules} \tag{13}$$

where M_s is the saturation magnetization, H_c is the coercive field, and V is the volume of the ferrite material. Thus, it can be seen that for low switching energies, each of these three parameters must be kept as low as is consistent with the requirements for satisfactory microwave operation.

3. SWITCH DESIGN

3.1 Switch Function and Configuration

A basic schematic of the ferrite latching switch is shown in Figure 9. This assembly contains 32 latching circulators, one fixed tuned circulator and 19 magic hybrid tees.

Latching circulators were designed in individual housings using OSM connectors. Each circulator has its own complete electronic driver board which permits the individual circulator to be removed from the main assembly. The electronic driver was constructed on a printed circuit board and is mounted remotely from the circulator.

The input circulators are arranged such that the output OSM connectors on the circulator will connect directly to the 180° magic tees to provide the best possible phase balance of the signals entering the magic tees. Figure 10 illustrates the manner in which the circulators and the magic tees are connected. The output of the magic tees (sum channel) are connected to the remaining circulator tree using semi-rigid MicroCoax 0.141 inches in diameter. Convenient lengths of this coax may be used since phase balance is no longer required. As may be seen from Figure 10, the magic tees are connected between the top and the bottom of every other circulator. This was done to best utilize the allotted space. The circulators were placed on 1" centers. The final outline dimensions of the switch assembly are 18 inches long, 10 inches deep and 5 inches high

3.1.1 Magic Tee Configuration

Many microwave applications require the use of so-called "hybrids," such as the matched magic tee and the hybrid ring or "rat race." Both of these devices may be represented by a symmetrical four-terminal pair network. Ideally[7], at the design frequency a matched load will be presented to any pair of input terminals provided the two adjacent terminal pairs are terminated in matched loads. In addition, power fed into these input terminals will divide equally between the two matched loads, and no power will appear at the fourth or opposite pair of terminals. The latter is commonly called the isolation arm.

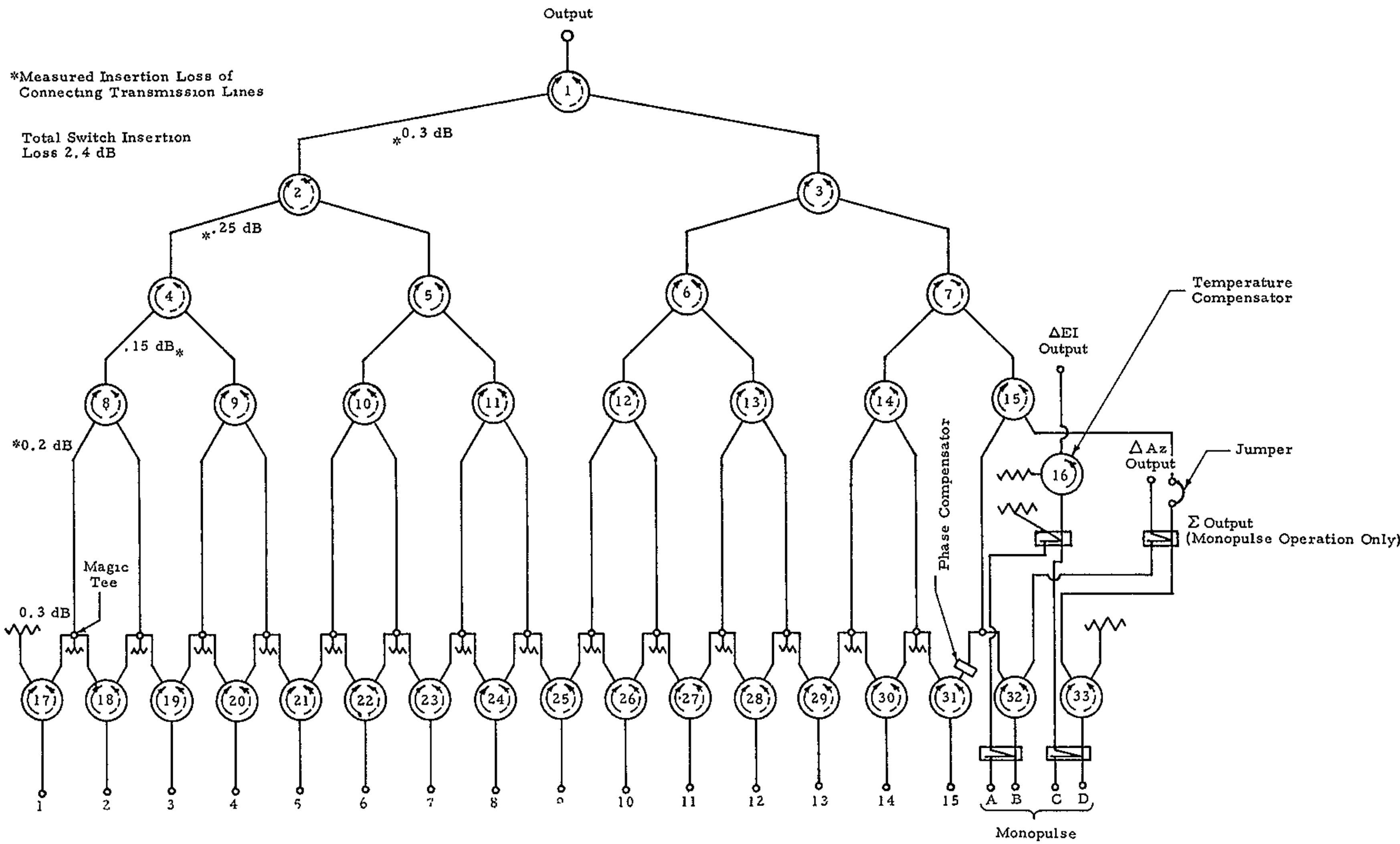

Figure 9. Latching Ferrite Switch for Beam Scanning (One Receiver)

In practice, the ideal is most nearly approached by the matched waveguide magic tee, since with this device good isolation and match are obtained over a relatively wide frequency band. However, where size is important and the power level is permissive, a shielded stripline hybrid ring can be used to good advantage. Such rings are fairly easy to design and build using a Z-Tron "G" dielectric material. Figure 11 illustrates the center conductor configuration of a shielded stripline hybrid ring.

Because the four arms are in parallel with the ring, it is necessary to make the characteristic impedance of the ring larger than that of the arms by a factor of $\sqrt{2}$ in order to obtain a reasonably good match over a broad frequency band. Unlike the matched waveguide magic tee, the isolation of a hybrid ring is a function of the electrical spacing of the arms and is, therefore, more frequency sensitive. Maximum isolation is obtained when the arm spacing is exactly equal to a quarter-wavelength, since the voltage incident on the isolation arm from one side of the ring is exactly equal in amplitude, but opposite in phase, to the voltage incident on that arm from the other side of the ring. Ideally, complete cancellation occurs and no power enters the isolation arm. In practice, junction effects and imperfect loads on the output arms prevent the realization of perfect isolation, irrespective of the type of transmission line used to make the ring.

Magic tees were constructed in this manner and the VSWR, isolation between undesired ports, and the insertion loss was maintained at approximately 1.1, 26 db, and 0.35 db, respectively.

3.1.2 Ferrite Programmer

Figure 12 is a photograph of the ferrite programmer illustrating the 16 position selector switch and the switch activate button.

The ferrite programmer contains logic selecting circuits as outlined in the electrical specifications, trigger generating circuits, a single channel selector switch and a manual control set button. Cable assemblies interconnect the trigger pulse generator with the microwave assembly.

FOLDOUT FRAME 1

FOLDOUT FRAME 2

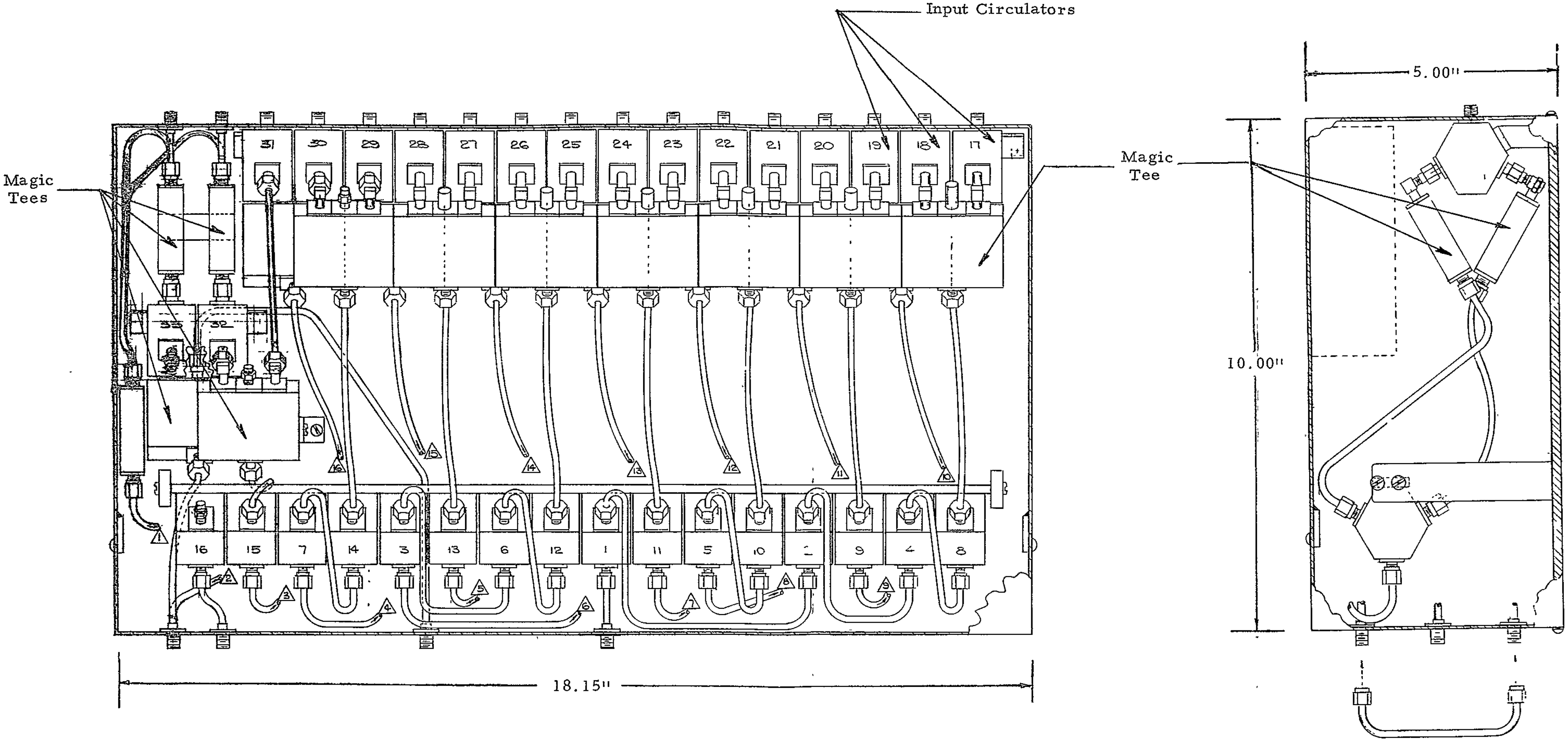

Figure 10. Drawing of the Microwave Portion of the Latching Ferrite Switch

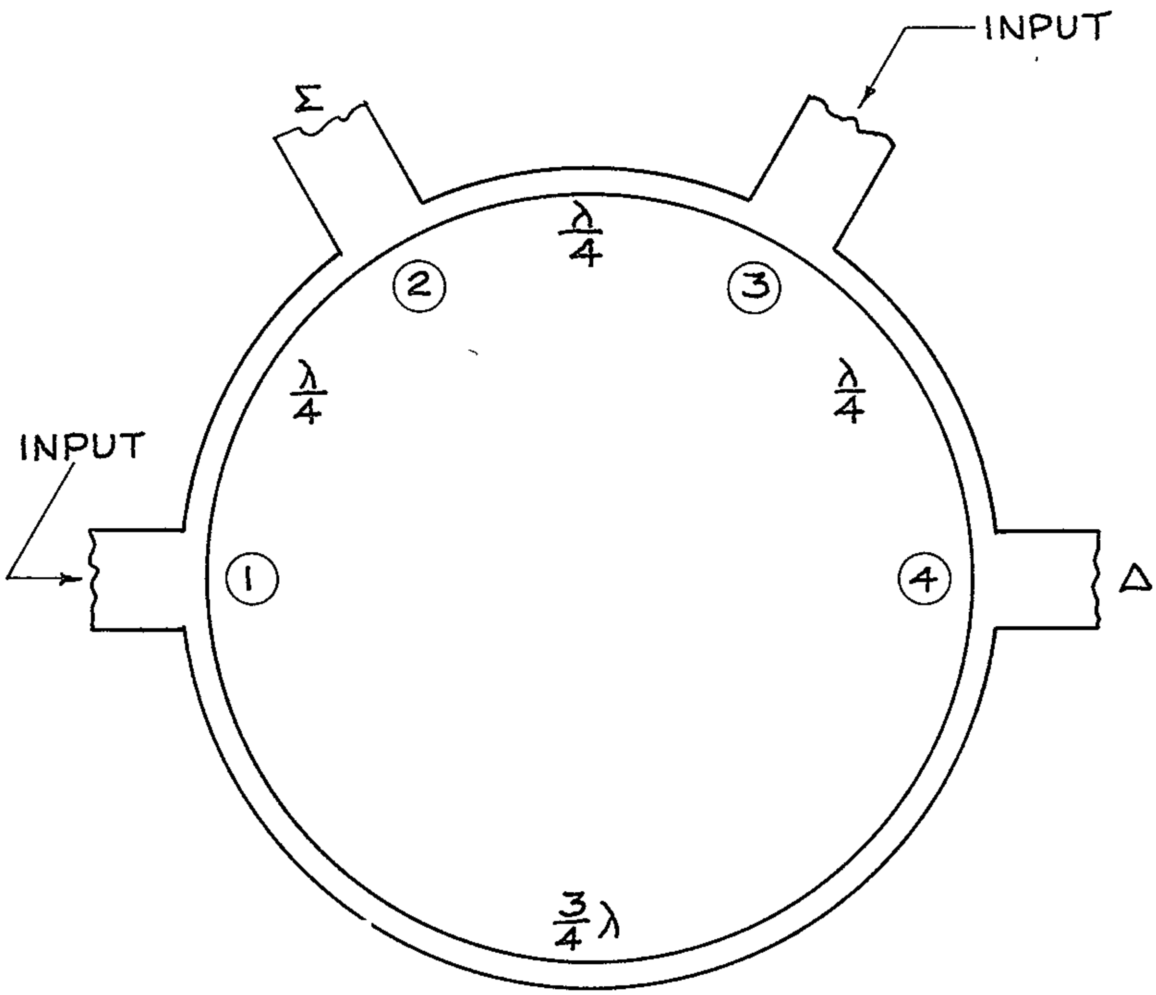

Figure 11. Center Conductor Design Used in a 180° Hybrid

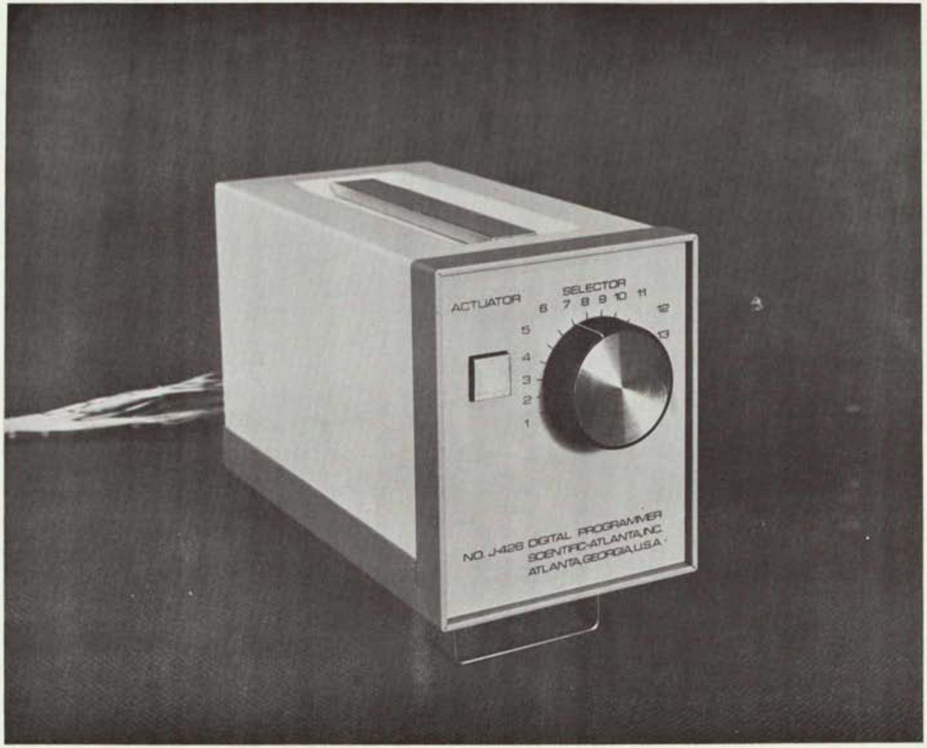

Figure 12. Photograph of the Ferrite Programmer

The system used for setting the direction of rotation of each circulator is basically a simple manually operated 16-position wafer switch as is shown in Figure 13.

The switching arrangement is similar to that encountered in the relay "tree" with the major exception being the fourth row of circulators (8 through 15). These circulators would normally select one of two possible inputs, and the whole row could be controlled by only two wafers. It is also desirable, however, to set the circulators to prevent undesired leakage paths between the input ports and the output port. To do this it is not only necessary to provide a path for the desired signal from input to output, but also to route all undesired signals back to the input ports to be lost either in the termination of the magic tees or to be reradiated at the input horns. This requires the use of additional wafers on the ganged switch but is necessary to insure the desired performance. Furthermore, in order to be able to accomplish this "rerouting" of undesired signals, the front row of circulators (#17-#33) must be placed alternately in CW and CCW positions. This is provided by the switching network.

To best illustrate the scheme of operation, a schematic diagram is shown in Figure 14 and a corresponding tabulation of circulator positions are shown in Table I.

The programmer consists of two main assemblies; the multi-pole multi-position selector switch and the trigger generator. The switch connects the pulse amplifier of the correct polarity to the input of each of the active circulators. The multi-position switch is wired in such a manner that each position will produce the right circulation in all the circulators which will have an effect on the insertion loss of the path from the desired pair of input ports to the output port. It should be noted that some of the circulators are switched even though they are not in the main path of energy; this is because they represent a possible leakage path that might interfere with the energy from the desired port.

The pulse amplifier (a block diagram is shown in Figure 15) consists of an "activate" push button, a bistable, and two pulse amplifiers, one inverting and one non-inverting. The activate push button latches the bistable into its "on" state when it makes contact upon operation.

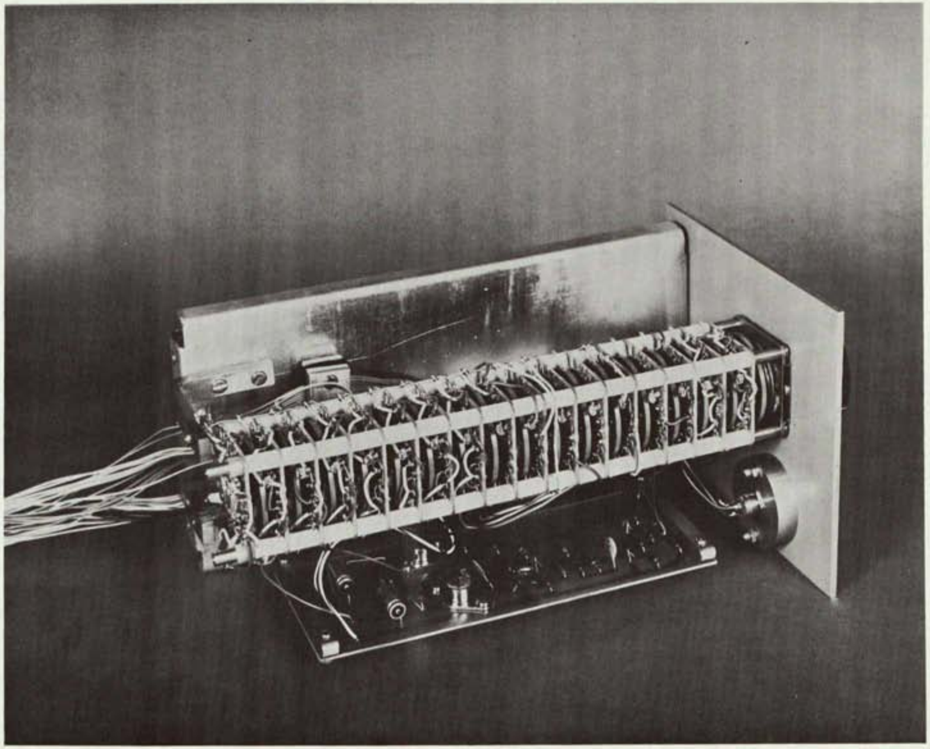

Figure 13. Exposed View of the Ferrite Programmer Showing the 16 Position Wafer Switch

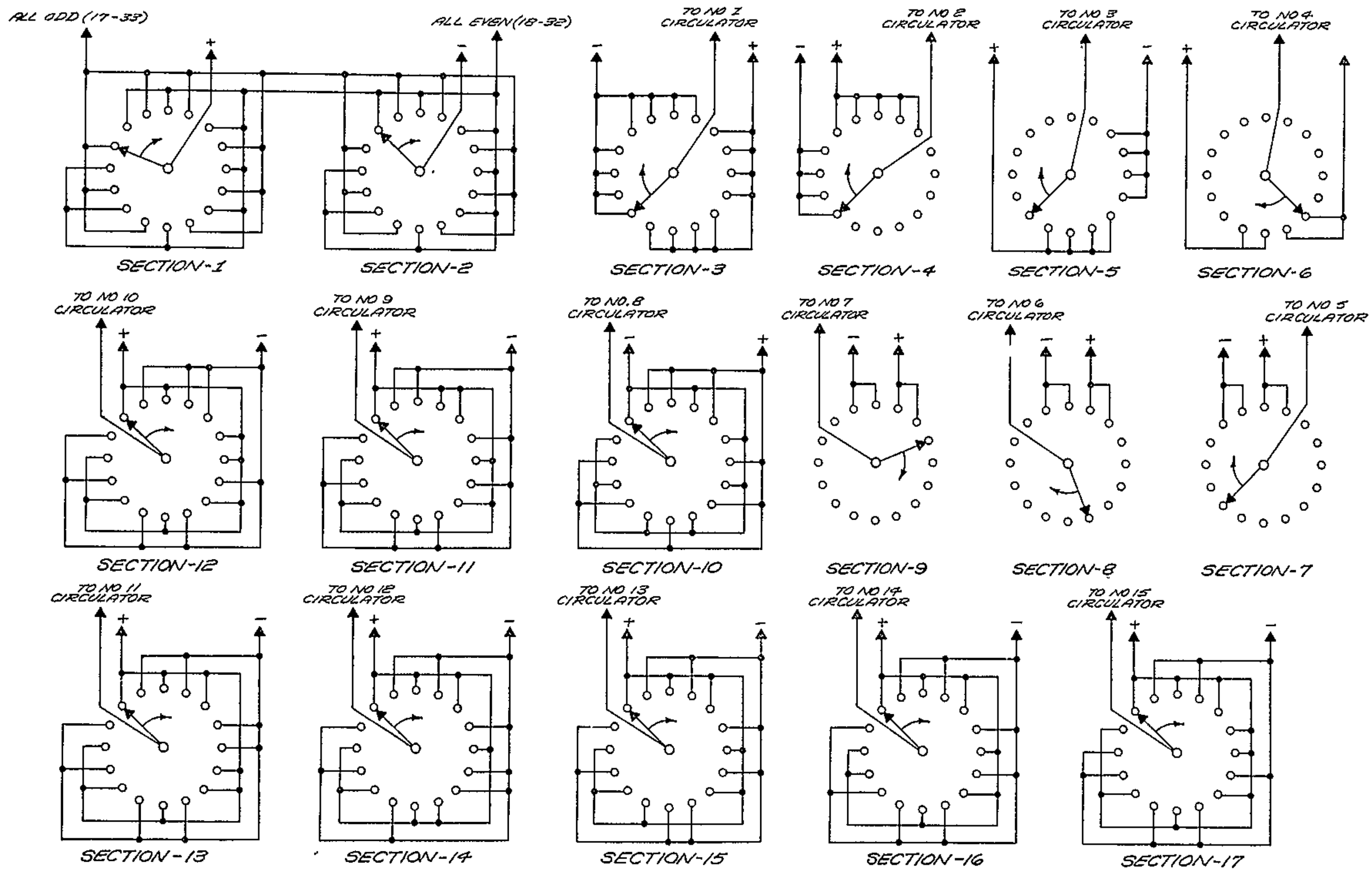

Circulator Direction
+ CCW   − CW

Figure 14. Schematic Diagram Illustrating the Connections to the 17-Section Wafer Switch within the Proposed Electronic Trigger Pulse Generator. All Wiper Arms Shown in Position 1.

Horns In Use	Circulator Number																															
	1	2	3	4	5	6	7	8	9	10	11	12	13	14	15	16	17	18	19	20	21	22	23	24	25	26	27	28	29	30	31	32	33
1, 2	A	A	O	A	O	O	O	A	B	B	B	B	B	B	B		B	A	B	A	B	A	B	A	B	A	B	A	B	A	B	A	B
2, 3	A	A	O	A	O	O	O	B	A	A	A	A	A	A	A		A	B	A	B	A	B	A	B	A	B	A	B	A	B	A	B	A
3, 4	A	A	O	B	O	O	O	B	A	B	B	B	B	B	B		B	A	B	A	B	A	B	A	B	A	B	A	B	A	B	A	B
4, 5	A	A	O	B	O	O	O	A	B	A	A	A	A	A	A		A	B	A	B	A	B	A	B	A	B	A	B	A	B	A	B	A
5, 6	A	B	O	O	A	O	O	B	B	A	B	B	B	B	B		B	A	B	A	B	A	B	A	B	A	B	A	B	A	B	A	B
6, 7	A	B	O	O	A	O	O	A	A	B	A	A	A	A	A		A	B	A	B	A	B	A	B	A	B	A	B	A	B	A	B	A
7, 8	A	B	O	O	B	O	O	B	B	B	A	B	B	B	B		B	A	B	A	B	A	B	A	B	A	B	A	B	A	B	A	B
8, 9	A	B	O	O	B	O	O	A	A	A	B	A	A	A	A		A	B	A	B	A	B	A	B	A	B	A	B	A	B	A	B	A
9, 10	B	O	A	O	O	A	O	B	B	B	B	A	B	B	B		B	A	B	A	B	A	B	A	B	A	B	A	B	A	B	A	B
10, 11	B	O	A	O	O	A	O	A	A	A	A	B	A	A	A		A	B	A	B	A	B	A	B	A	B	A	B	A	B	A	B	A
11, 12	B	O	A	O	O	B	O	B	B	B	B	B	A	B	B		B	A	B	A	B	A	B	A	B	A	B	A	B	A	B	A	B
12, 13	B	O	A	O	O	B	O	A	A	A	A	A	B	A	A		A	B	A	B	A	B	A	B	A	B	A	B	A	B	A	B	A
13, 14	B	O	B	O	O	O	A	B	B	B	B	B	B	A	B		B	A	B	A	B	A	B	A	B	A	B	A	B	A	B	A	B
14, 15	B	O	B	O	O	O	A	A	A	A	A	A	A	B	A		A	B	A	B	A	B	A	B	A	B	A	B	A	B	A	B	A
15, A+B	B	O	B	O	O	O	B	B	B	B	B	B	B	B	A		B	A	B	A	B	A	B	A	B	A	B	A	B	A	B	A	B
A+B, C+D	B	O	B	O	O	O	B	A	A	A	A	A	A	A	B		A	B	A	B	A	B	A	B	A	B	A	B	A	B	A	B	A
Wafer #	3	4	5	6	7	8	9	10	11	12	13	14	15	16	17		← Controlled by two wafers -- 1, 2 →																

Note: A = CW
B = CCW
O = Not Significant

Table I. Switching Circulator Position Chart

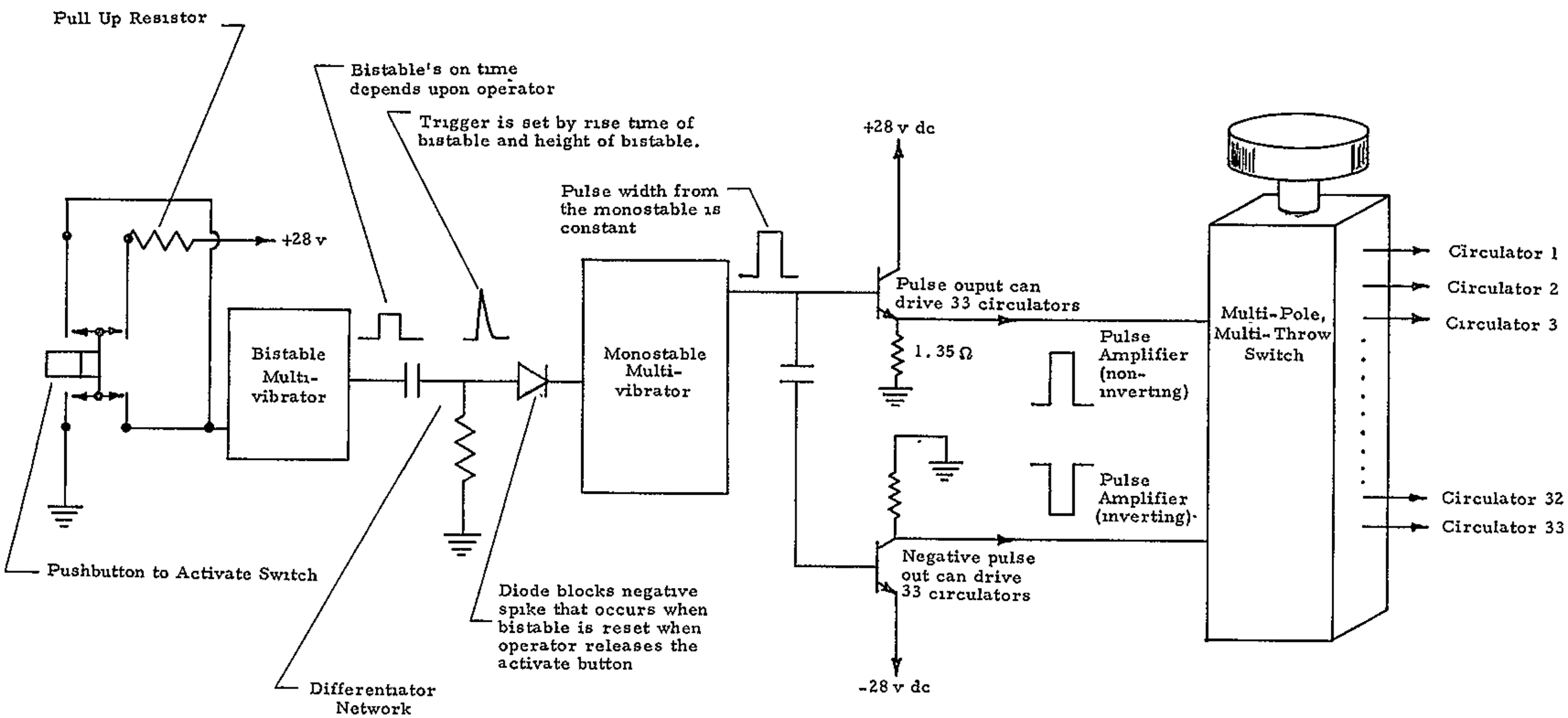

Figure 15, Block Diagram of the Ferrite Programmer.

The output of the bistable is a steep rising pulse which is differentiated. This pulse is used to trigger a monostable multivibrator which puts out a flat topped drive pulse of the desired duration to drive the two output amplifiers. The two amplifiers are high current, high frequency power transistors which can drive all of the wiring capacity and the input loading of the 33 circulators which must be switched simultaneously. The schematic diagram of this circuit is shown in Figure 16.

3.1.3 Circulator Driver Circuit

A schematic diagram of the driver circuit for one latching circulator is shown on the following page on Figure 17. This circuit was especially designed for this application to reduce the number of interconnecting cables required and to trigger each circulator from a simple fast rise time trigger.

A single input trigger terminal will be supplied on the circulator to accept the switching pulses required to initiate a change in the direction of circulation. To make this possible, the pulse circuits are polarity sensitive with positive pulses setting the circulator rotation CCW and negative pulses setting the circulator for CW rotation.

Each circulator contains its own pulse shaping circuitry which is factory adjusted for optimum response. This is accomplished using a two-transistor one-shot pulse generator for each direction of rotation. The CCW one-shot multivibrator is driven directly from the input pulse, while the CW one-shot multivibrator is driven by a pulse inverter stage. The inputs to the one-shot multivibrators are isolated from the line and from each other with suitable diodes and capacitors. The pulse produced by the one-shot multivibrator is applied to a high current driver which can pass up to 10 amperes through the magnetizing winding of the ferrite core. This transistor must also be able to withstand an inductive surge of approximately 70 volts when the current is cut off. Cut-off is determined by the width of the input pulse from the multivibrator which is relatively constant.

One very significant feature of this design is that a current sensing circuit is included to prevent excessive switching energy should the circulator be switched twice in succession in the same direction. Without such a sensing circuit, a

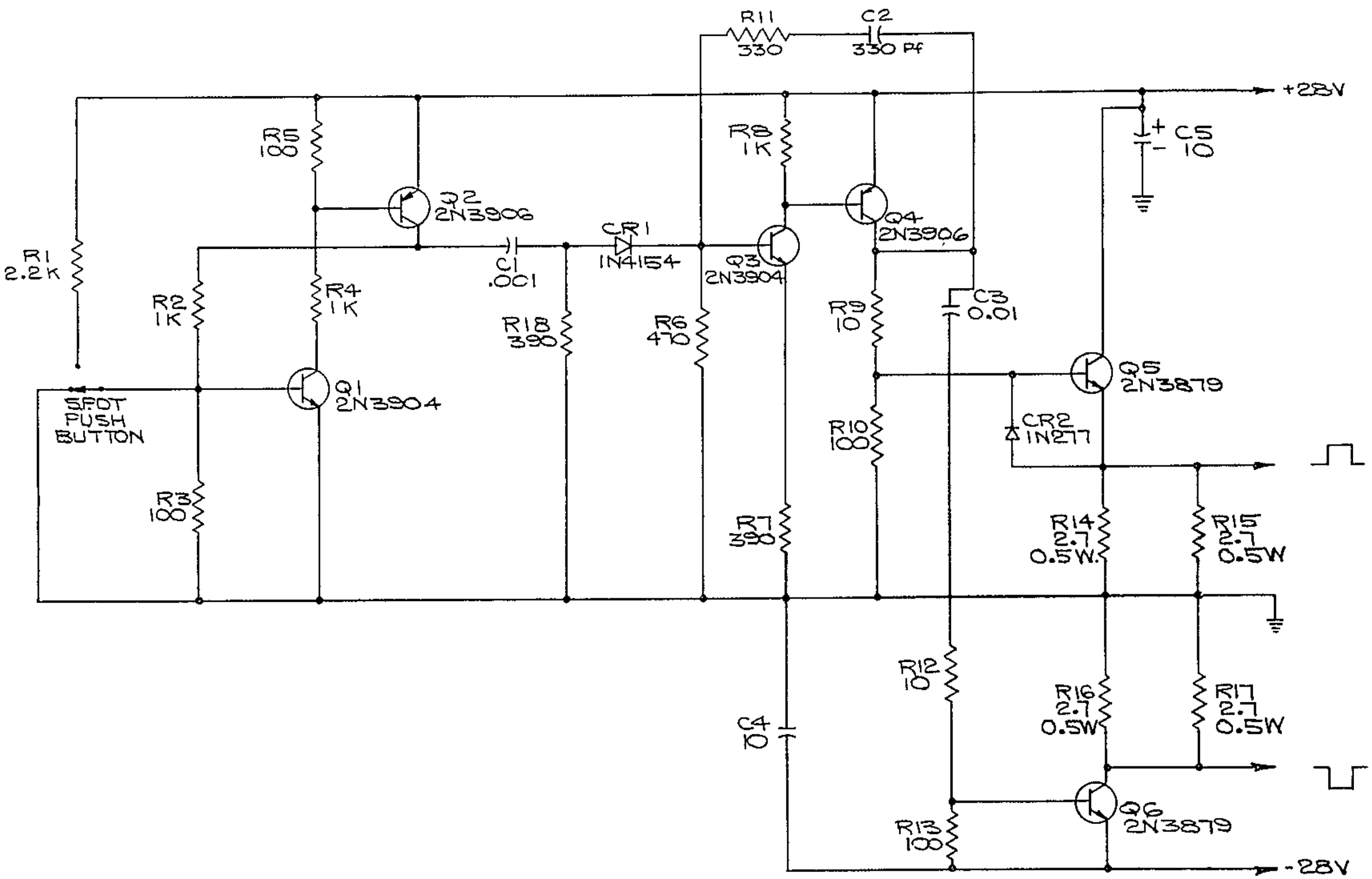

Figure 16. Schematic Diagram of the Ferrite Programmer.

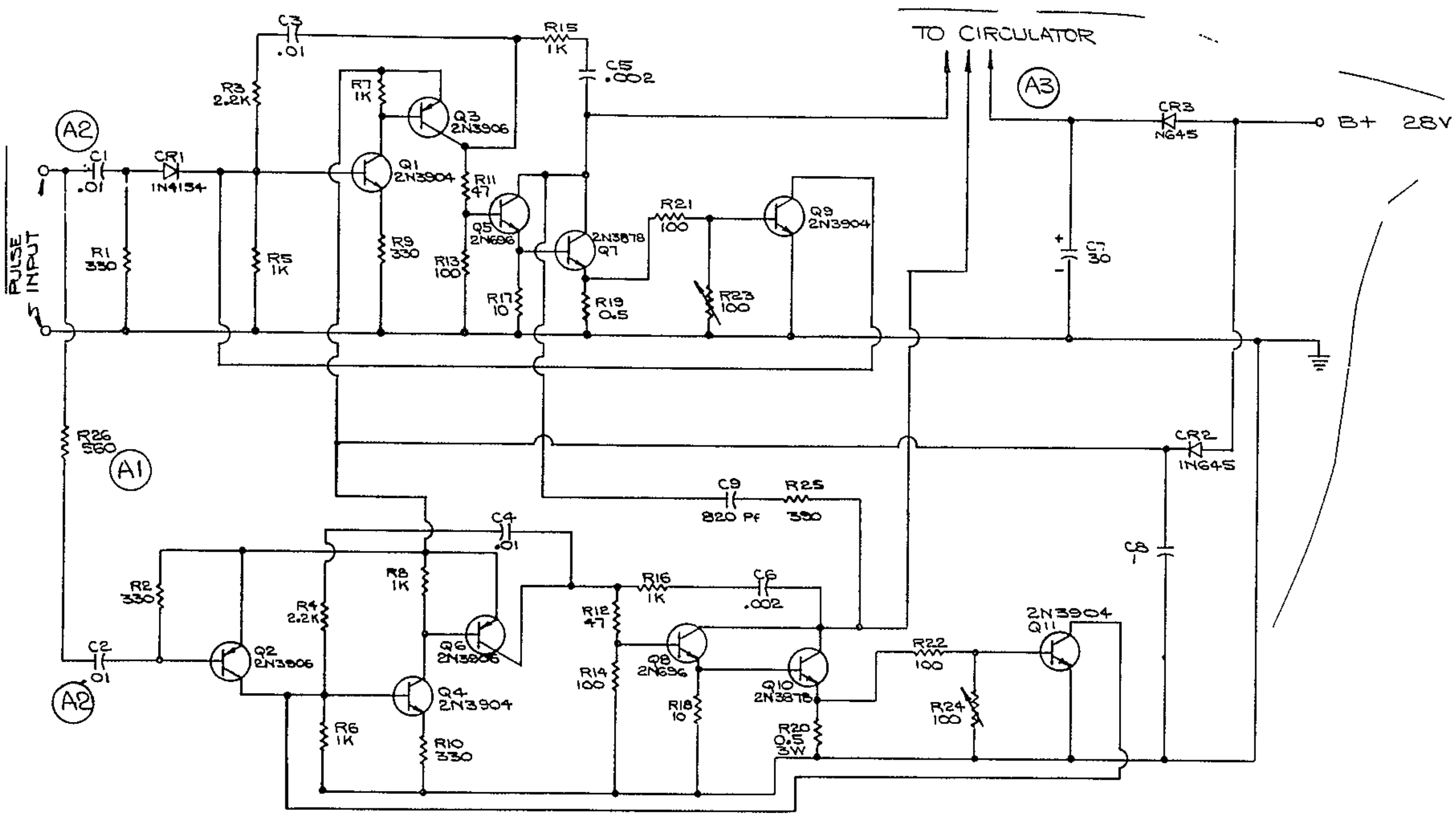

Figure 17. Schematic Diagram of the Latching Circulator Driver Circuitry

latching circulator switched twice in the same direction will require four to five times as much energy as it would have for a normal switching operation. If the circulator has been set in the desired state and a second pulse is received to again set it into the same state, the current will rise much more rapidly than usual and, hence, considerably more energy will be consumed. To prevent this, a sensing resistor is added to the emitter of each high current driver transistor (Q7 and Q10). The voltage drop across this resistor is used to drive a transistor into conduction which in turn is connected back into the pulse generator in such a manner as to cause the pulse to be cut off as soon as the current rises to a value sufficient to insure magnetization.

The circulator is isolated from the power supply circuits by surge limit resistors and the main driver circuit is isolated from the pulse generator circuit. This will permit a large number of circulators to be operated on a common power supply without danger of mutual interaction. When a large number of circulators switch simultaneously, there is a heavy load applied to the power supply to recharge the condensors. This could cause an immediate switching request to not be satisfactory if it followed such a step; therefore, a large common capacitor is located in the cabinet close by the switching boards to maintain local B plus close to the supply voltage.

A photograph of the completed latching circulator driver is shown in Figure 18, along with a latching circulator. One such driver board weighs approximately 1.75 ounces.

3.1.4 Latching Circulator Configuration

The basic structure used to provide the required microwave SPDT switches is a latching stripline circulator. The techniques involved in the development and construction of devices of this kind were discussed in detail in Sections 2.1 2.2 and 2.3.

Figure 19 illustrates schematically the design of the X-band stripline latching circulators. As may be seen in this figure, the microwave junction itself is extremely small, being on the order of one-half inch in diameter and one-eighth

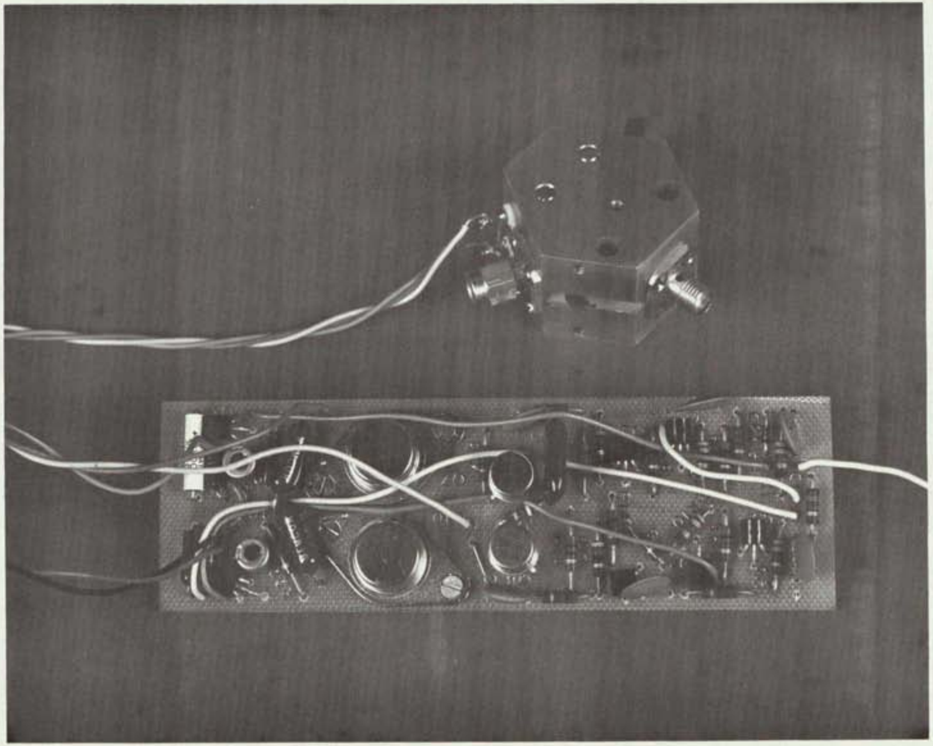

Figure 18. Photograph of the Completed Latching Circulator Driver, Along with a Latching Circulator

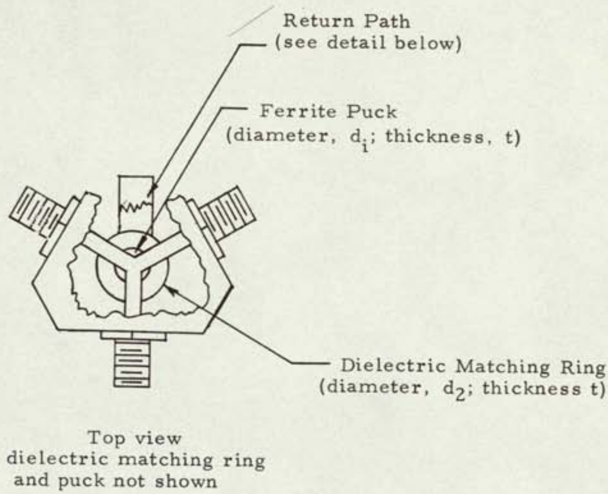

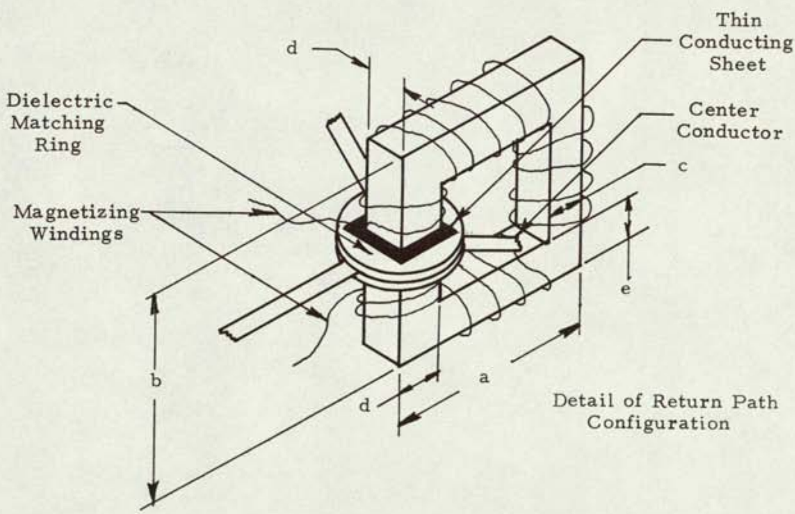

Figure 19. Schematic of the X-Band Latching Ferrite Circulator

inch high. Table II outlines the physical dimensions of the latching circulator. In addition to the overall weight of the latching circulator, the weight of the microwave components alone (i.e. weight of the device minus that of the aluminum ground planes and the RF connectors) has been listed. This was done to give an indication of the weight which might be expected if the device were constructed in an integrated circuit configuration.

Physical Dimensions of Entire Unit	approx. 1.5" x 1.5" x 1" excluding connectors
Overall Weight (Excluding Driver)	2.5 ounces
Weight of Microwave Components (Excluding Driver, Ground Planes and Connectors)	0.6 ounces
Dimensions of Ferrite Puck, d_1, t	0.300" dia. x 0.063" high
Dimensions of Dielectric Matching Ring, d_2, d_1, t	0.605" OD x 0.300" ID x 0.063" high
Dielectric Constant of Matching Ring	6.5
Dimensions of Return Path (see Figure 19)	
a	0.775"
b	0.900"
c	0.300"
d	0.300"
e	0.217"

Table II. Physical Dimensions of the X-Band Latching Circulator

3.1.4.1 Design Considerations

The microwave junction was designed utilizing the equations and graphs presented in Section 2.2. The ferrite puck was fabricated from Trans-Tech 1-390 which has a saturation magnetization of 2150 gauss; the outside diameter of the puck was made to be 0.300". Both of the values are in agreement with those predicted by the graph in Figure 5 for a center frequency of 8.0 GHz.

The impedance transforming network selected to provide a match between the 50 ohm input transmission line and the ferrite junction impedance (approximately 13 ohms) was a two-step quarter wave transformer. The exact configuration of these transformers can be seen in Figure 20, a photograph of the microwave configuration taken after removing the upper ground plane, ferrite puck, and dielectric ring. As may be seen, the width of the stripline is reduced above the dielectric ring in order to make the characteristic impedance of this section the correct value to achieve the desired impedance transformation. The length of this reduced width section (d_2 - d_1) in Figure 19 was made to be one quarter of a wavelength in the dielectric constant of the ring (6.5) at the center frequency of operation.

The magnetic return path is completely shielded from the microwave energy by the thin conducting sheets (Figure 19) which are placed on both the top and bottom sides of the microwave junctions. These sheets and the microwave center conductor were made as small as possible to reduce eddy current losses when the composite toroid is switched. At the same time, these sheets serve as the ground planes and center conductor of the microwave junction and hence cannot be made arbitrarily thin without giving rise to high microwave insertion loss. For this reason, the conducting sheets were made to be approximately two skin depths at the microwave frequency. This seems to represent a satisfactory compromise between switching and microwave considerations.

Since the external return path (Figure 19) is completely shielded from the microwave energy, it is not necessary to select a ferrite having good microwave properties. For this reason, a lithium ferrite Trans-Tech L-6 was chosen. This material has excellent hysteresis and temperature properties as shown in Table III below.

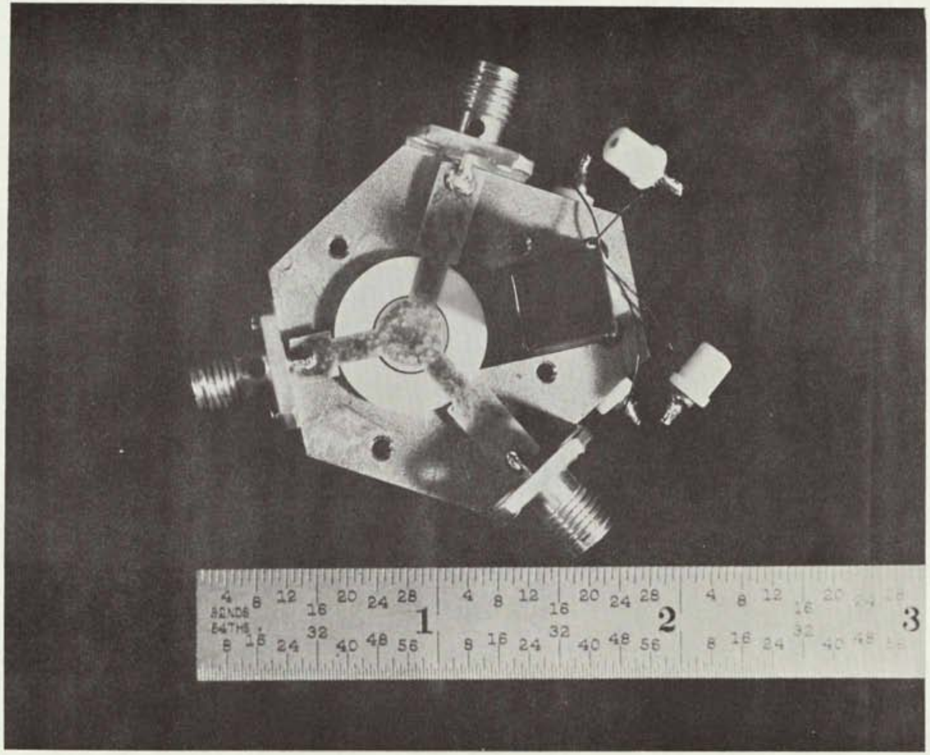

Figure 20. Photograph of an X-Band Latching Circulator with the Top Section Removed

$4\pi M_s$	3435 Gauss
B_m	2978 Gauss
B_r	2686 Gauss
H_c	4.36 Oersted
S (squareness ratio $= \frac{B_r}{B_m}$)	0.9
T_c	~560°C

Table III. Properties of the Lithium Ferrite Material Used in Fabricating the External Return Path

Although the temperature properties of the particular material batch used was not measured, Figure 21 illustrates the temperature variation of B_m, B_r, and H_c for another batch of the same material. As may be seen, little variation in these properites is observed over the desired temperature range of -20°F (-28.9°C) to 125°F (51.6°C).

The dimensions of the return path are shown in Figure 19 and Table II; these were determined with the aid of the relationships discussed in Section 2.3.

3.1.4.2 Microwave Performance

Since the required bandwidth (7.9 - 8.1 GHz) was relatively narrow, no difficulties were experienced in maintaining the required isolation and insertion loss once the microwave junction and impedance matching network had been optimized. To illustrate this, a swept frequency plot of insertion loss and isolation for a typical unit is shown in Figure 22. It will be noted that both the isolation and insertion loss remain quite flat over the required band. For this reason, the measured values of isolation and insertion loss at the center frequency serve as a good indicator of overall device performance. (All of the 33 latching circulators exhibited more than 20 dB isolation and less than 0.3 dB insertion loss

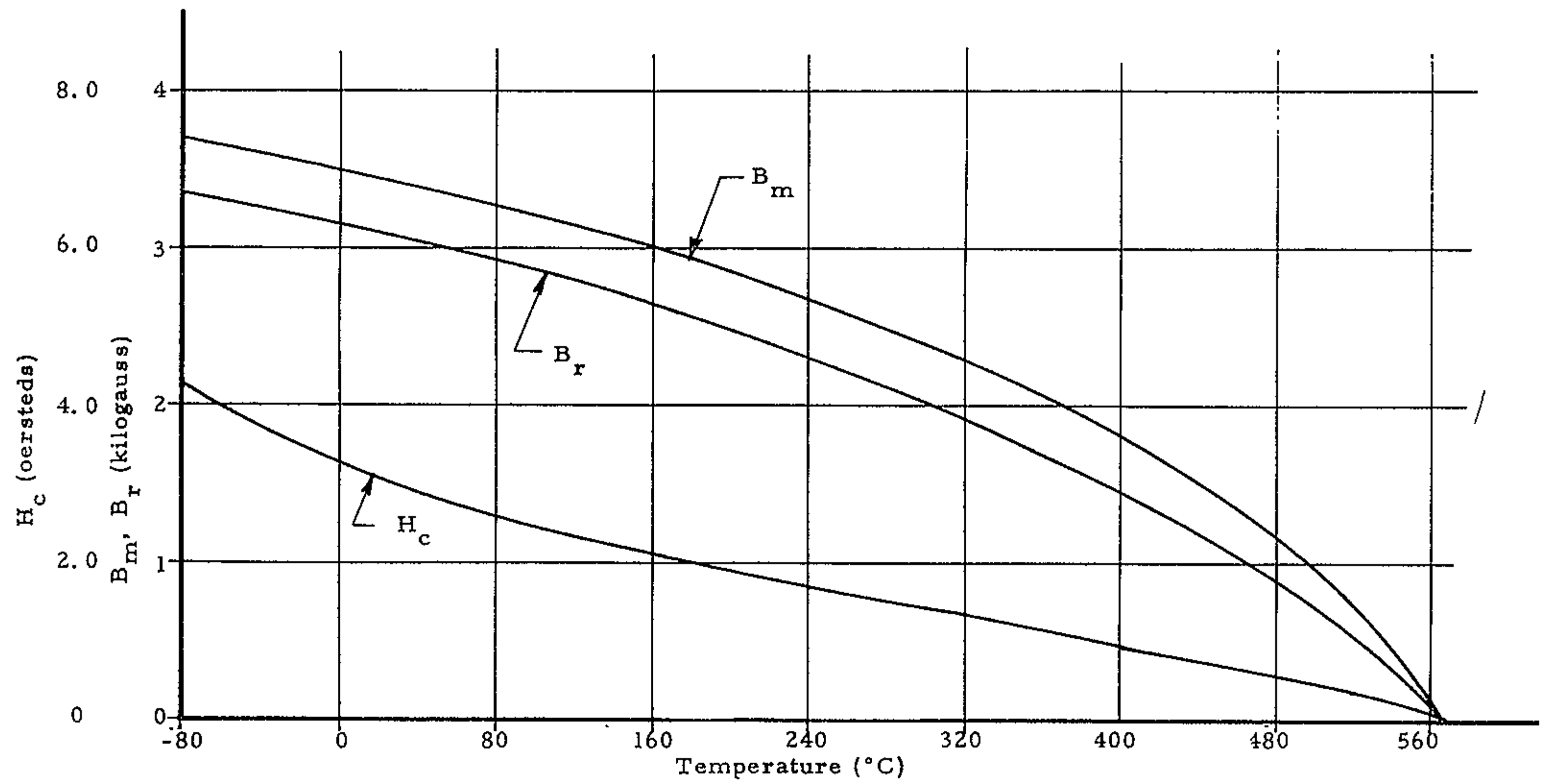

Figure 21 Temperature Variation of the Hysteresis Properties of a Lithium Ferrite Similar to that Used in Fabricating the External Return Paths for the X-band Latching Circulators.

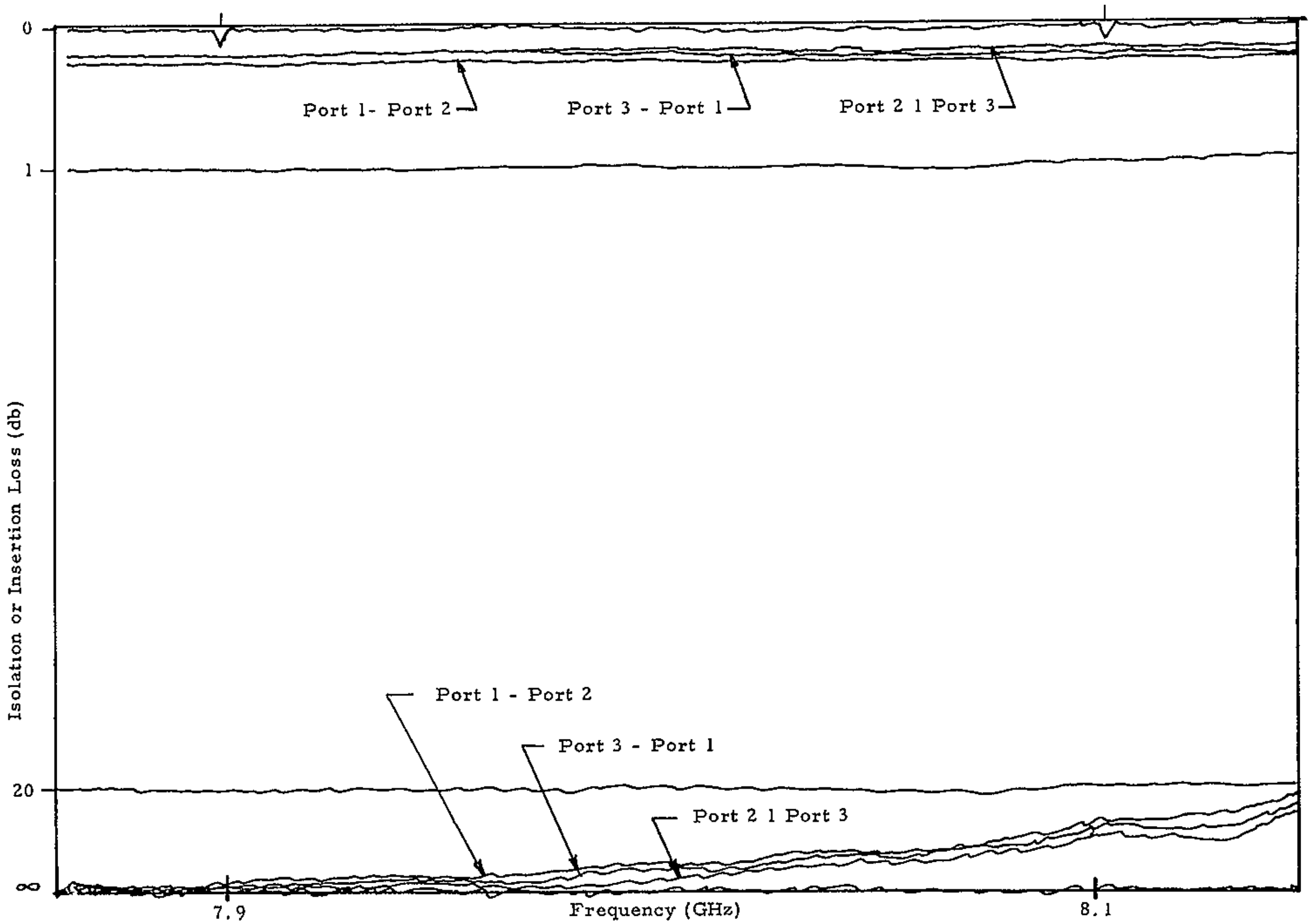

Figure 22. Swept Frequency Plot of Insertion Loss and Isolation of a Typical Ferrite Latching Circulator (S. P. D. T.).

over the required band). Table IV gives the measured microwave properties at 8.0 GHz for each of the 33 units, along with the switching energy and time.

Also shown in Table IV are the values of switching energy and switching time. As may be seen, the switching energy typically falls between 2000 and 3000 microjoules, and the switching time typically falls between 20 and 30 microseconds. The rather large variation in switching energy is attributed to variation of the thickness of the conducting film used to form the microwave center conductor at the point where these elements intersect the composite toroid. A thicker conducting surface would lower the resistance of the "shorted-turn" effectively presented to the toroid, and hence would increase both the switching energy and time.

Table V contains the insertion phase (in both of the possible switching states) measured on each of the 17 latching circulators used at the input terminals, and in the monopulse section of the switch. It was required that insertion phase of these remain quite close from unit to unit in order to assure proper summing at the magic tee power combiners and/or proper operation of the monopulse circuitry.

The maximum deviation of the insertion phases from the population mean is 7.3°. It is only necessary (with the exception of those circulators in the monopulse section) that adjacent signal paths feeding the same magic tee have the same insertion phase. That is (considering Figure 9) one needs to make the insertion phase seen by a signal entering Port 1 of the switch passing through Circulator 17 and then into the magic tee, close to that insertion phase seen by a signal entering Port 2 of the switch, traveling through Circulator 18 and into the same magic tee. Thus it is required only that adjacent signal paths have the same insertion phase, and as a result it was possible by proper selection of the circulators used at each of the input ports to provide an even better phase match than that shown above.

The variation of insertion phase with frequency measured on five randomly selected units is shown in Figure 23. As may be seen, over the range of -20 to 125°F, all of the units measured fell within the required ±5° envelope. The use of two data points at room temperature is due to the fact that these

CIRCULATOR CHARACTERISTICS
at 8.0 GHz

CIRCULATOR REFERENCE NO.	ISOLATION (db)	INSERTION LOSS (db)	SWITCHING TIME (μsec)	SWITCHING ENERGY (μjoules)
1	28	.15	30	2690
2	25	.15	30	2900
3	28	.25	30	2680
4	22	.20	30	2461
5	23	.30	25	2350
6	30	.15	30	2690
7	25	.20	25	2580
8	25	.30	25	3020
9	22	.20	25	1790
10	23	.20	25	2800
11	25	.15	25	2460
12	30	.15	30	2280
13	23	.25	20	1680
14	28	.20	25	2690
15	23	.20	25	2130
16	30	.20	20	1565
17	32	.25	25	2460
18	22	.30	20	2120
19	22	.30	25	2580
20	25	.20	30	2350
21	22	.20	30	3020
22	25	.25	25	2800
23	23	.20	30	3020
24	25	.30	30	2910
25	23	.20	25	3590
26	28	.25	30	2810
27	23	.20	20	2690
28	25	.25	25	3020
29	28	.20	25	3020
30	24	.25	30	2240
31	28	.25	25	3360
32	30	.20	30	3140
33	25	.25	25	2900

Table IV

VARIATION OF INSERTION PHASE FROM UNIT TO UNIT

UNIT NO.	DIRECTION of CIRCULATION PORT # - PORT #	INSERTION PHASE	DEVIATION FROM MEAN
1	1-2	35.9	-7.3°
1	1-3	44.7	1.5
2	1-2	44.3	1.1
2	1-3	46.2	3.0
3	1-2	44.0	.8
3	1-3	42.9	- .3
6	1-2	46.6	3.4
6	1-3	48.0	4.8
7	1-2	45.7	2.5
7	1-3	41.8	-1.4
8	1-2	45.4	3.2
8	1-3	47.9	4.7
9	1-2	47.0	3.8
9	1-3	48.1	4.9
10	1-2	41.0	-2.2
10	1-3	45.0	1.8
12	1-2	43.2	0
12	1-3	42.6	- .06
13	1-2	47.6	4.4
13	1-3	42.6	- .06
15	1-2	47.6	4.4
15	1-3	43.9	.07
17	1-2	38.2	-5.0
17	1-3	40.1	-3.1
18	1-2	47.8	4.6
18	1-3	50.0	6.8
23	1-2	43.4	.02
23	1-3	40.9	-2.3
26	1-2	47.0	4.8
26	1-3	45.4	2.2
27	1-2	43.2	0
27	1-3	42.0	-1.2
28	1-2	44.7	1.5
28	1-3	44.8	1.6

Table V

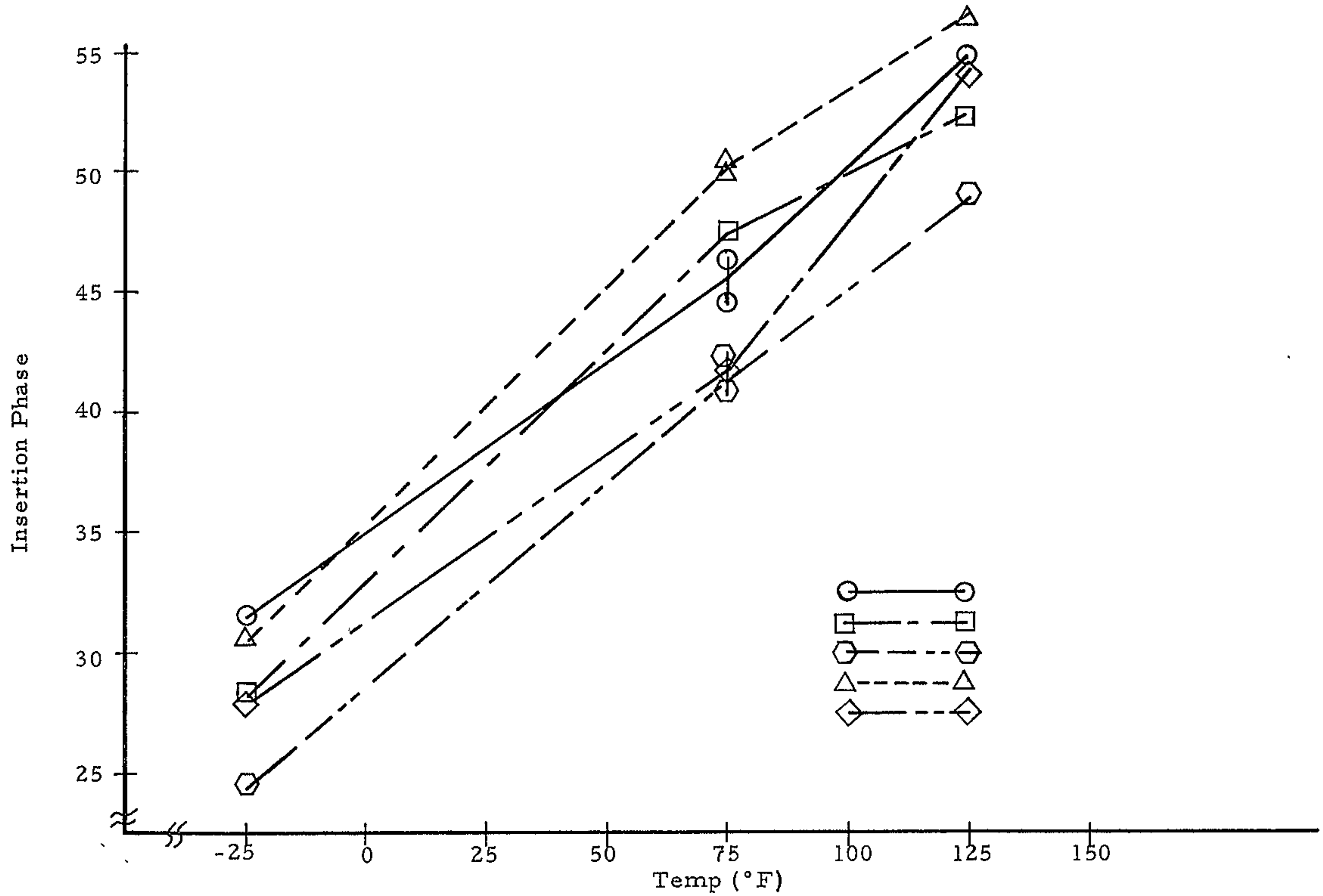

Figure 23. Variation of Insertion Phase vs. Temperature for Five Randomly Selected Latching Circulators.

measurements were made twice, once before the high and low temperature measurements, and once after. The difference in these two sets of measurements give a good indication of the accuracy of the measuring system. The largest discrepancy in the room temperature measurement was only 2°.

3.2 Switch Performance

Figure 24 shows the final internal assembly of the switch exposing the circulators, magic tees, electronic drivers, and cabling, and Figure 25 illustrates the external appearance of the completed switch.

A considerable amount of swept frequency data was taken on the assembled unit. Due to the similarity of data taken for each of the sixteen possible switch settings, typical data will be presented in this report. Figure 26 illustrates the isolation and insertion loss for a particular setting of the switch (in this case it is set to select an input to Ports 14 and 15) for signals applied to various inputs. Since this switch network is constructed so as to combine the signals in two of the inputs, in all of these measurements, signals of equal amplitude and phase were applied to two adjacent terminals. This power splitting was accomplished by inserting a magic tee between the generator and the ports to which power was to be applied; the particular tee used was of the same type as those described in Section 3.1.2 except it had been selected to have extremely good amplitude and phase balance.

When one of the ports to which an input was applied was one of the two pairs of monopulse inputs, it was necessary to use additional magic tees to split the power applied to this port between its upper and lower connectors (i.e., ports A and B for input 16 and ports C and D for input 17).

In Figure 26, the low loss curve is that measured when power of equal amplitude and phase was applied to Ports 14 and 15. The curves having higher loss represent similar balanced inputs to 1 and 2; 2 and 3;.....11 and 12; 12 and 13; and finally (A + B) and (C + D). As was stated above, in all cases, the switch was set to receive power applied to Ports 14 and 15. As may be seen, the isolation for each of the undesired inputs exceeds 30 dB. In actuality, the isolation in most cases was probably in excess of 40 dB, but the noise level of the measure-

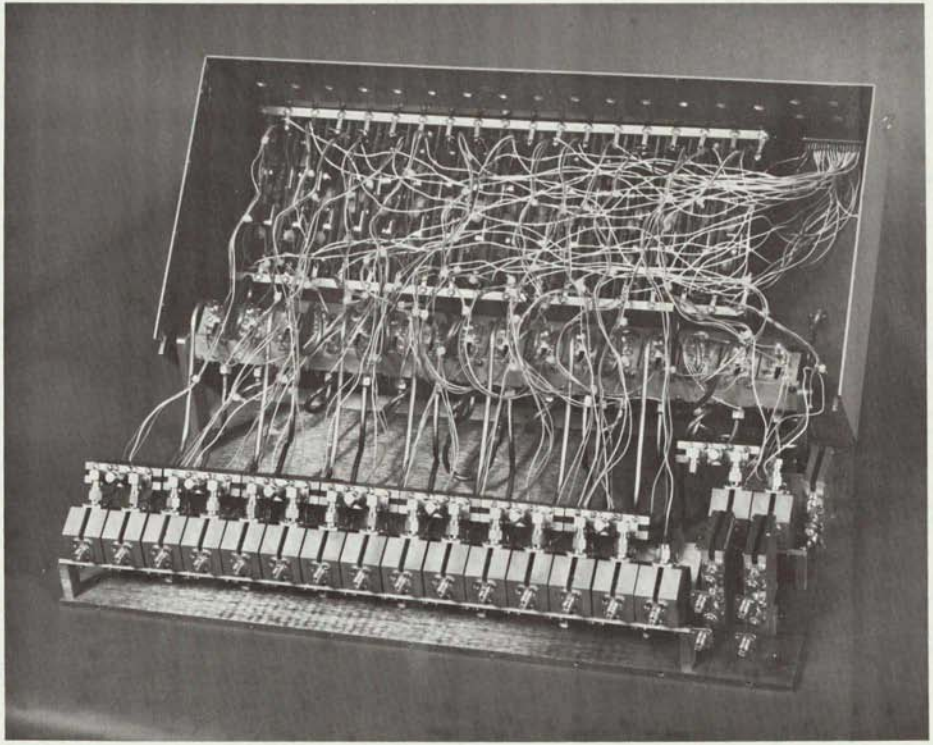

Figure 24. Photograph of the Completed Switch Assembly with Top Removed

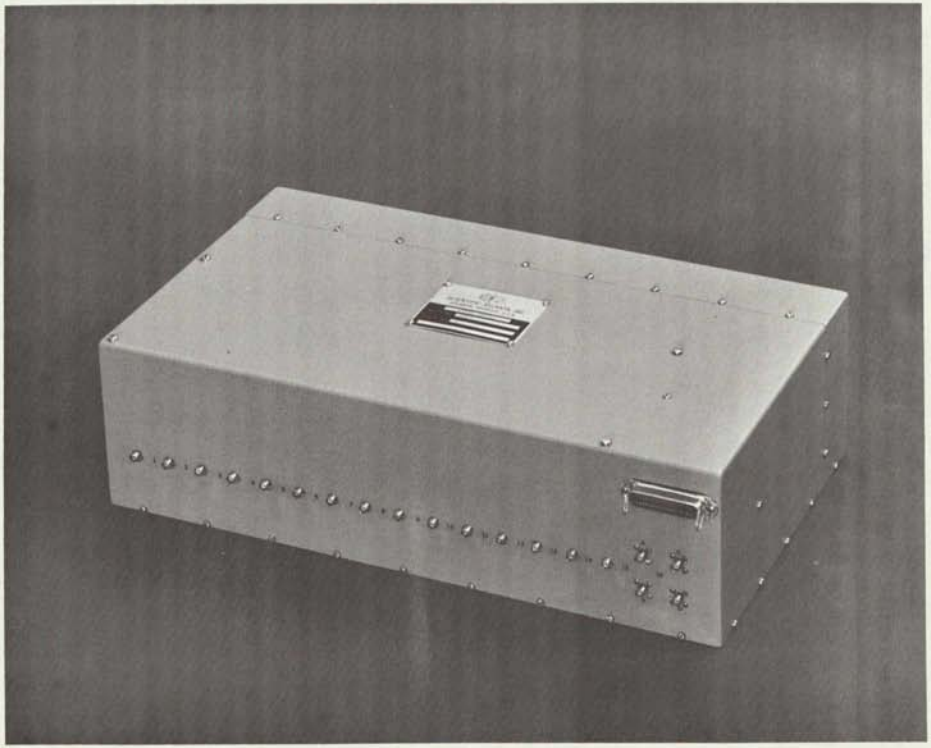

Figure 25. Photograph of the Completed Switch Assembly

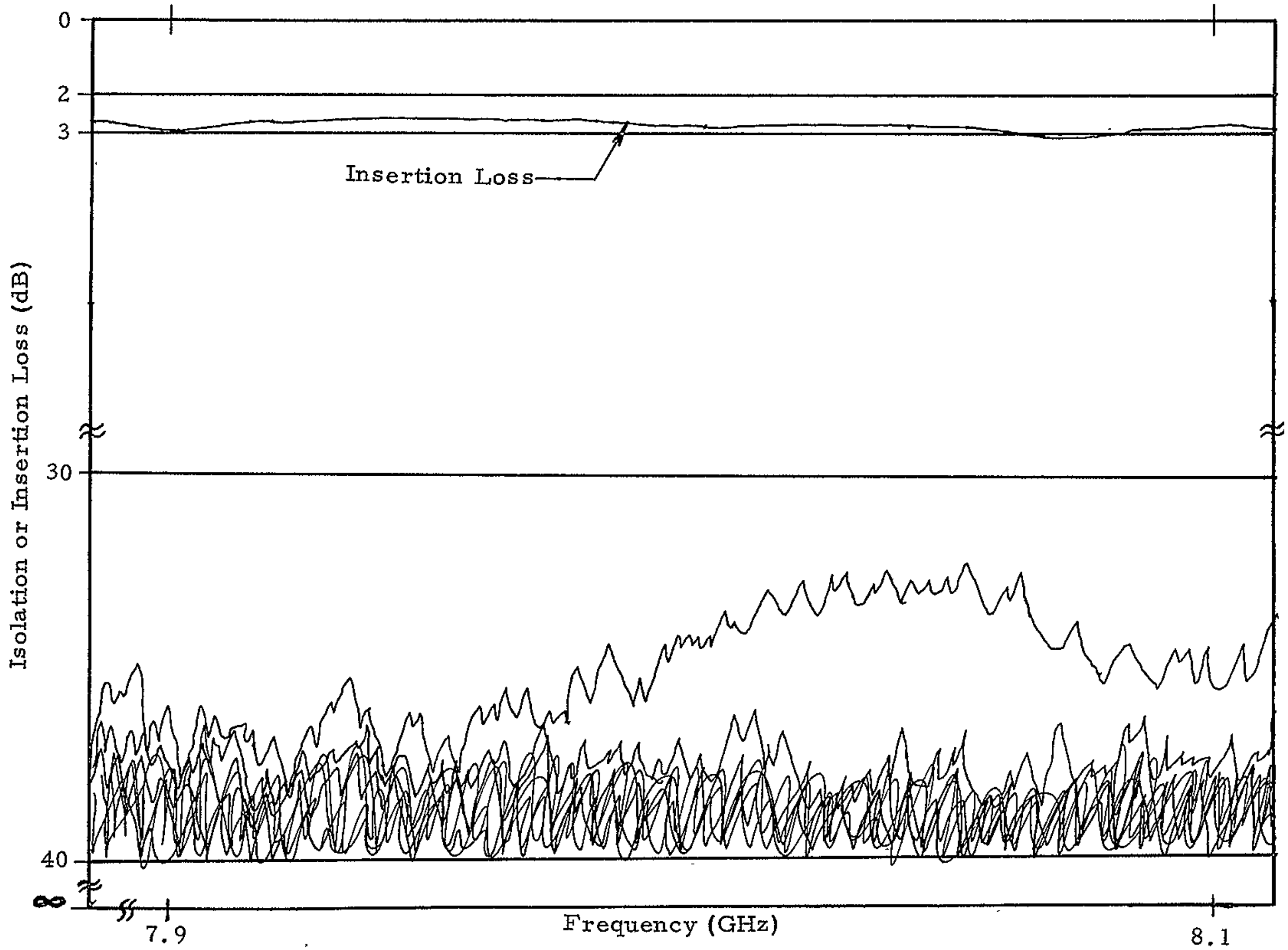

Figure 26. Swept Frequency Plot of Isolation and Insertion Loss with the Switch Set to One of its Possible Receive Positions.

ment system prevented measurement of isolations greater than about 37 dB. The insertion loss is seen to be typically less than 3.0 dB. It should be noted, however, that of this loss 0.5 dB is accounted for by the d.c. block located at the output of the switching matrix, and hence only 2.5 dB is due to the switch itself.

The frequency variation of input VSWR is illustrated in Figure 27. Each of the curves were measured by applying an input signal to one of the 18 input ports and measuring the relected power when the switch was set to receive from the port being tested. It may be seen that the input VSWR remains less than 1.30 in all cases, and typically remains well below 1.25.

Figure 28 shows the effect of ambient temperature upon isolation and insertion loss. These performance characteristics were obtained using the same technique as used in obtaining Figure 26, except that the isolation is only shown for one typical port. As may be seen, the isolation remains well below 30 dB over the required temperature range. The insertion loss, on the other hand, increases somewhat at the low temperature extreme. This increase in loss does not seem to be attributable to losses in the circulator. It is possible that this increase is due to increased losses in the interconnecting cables or possibly is a measurement error introduced by the necessity of using flexible cables in making the low temperature measurements.

Swept frequency plots of the monopulse performance characteristics are shown in Figure 29. These were measured while applying four signals, each having equal amplitude and phase to the four monopulse inputs (A, B, C, and D shown in Figure 9). In making the sum channel measurements the monopulse jumper cable was removed and the signal out of the sum channel was compared to the total power applied to the four monopulse inputs. As may be seen the insertion loss in the sum channel remains less than 1 db over most of the band. The output signal from the two error channels (azimuth and elevation) should indicate difference in phase between the signals applied to the four monopulse inputs (i.e., $\Delta Az = (A + B) - (C + D)$ and $\Delta El = (A + C) - (B + D)$). Hence, when these outputs are measured with signals equal in both amplitude and phase applied to inputs A, B, C, and D, the output signals from both of the error channels should be well below the total energy applied to the inputs. Figure 29 shows that this is the case, both of these outputs being isolated by greater than 25 db over the required frequency band.

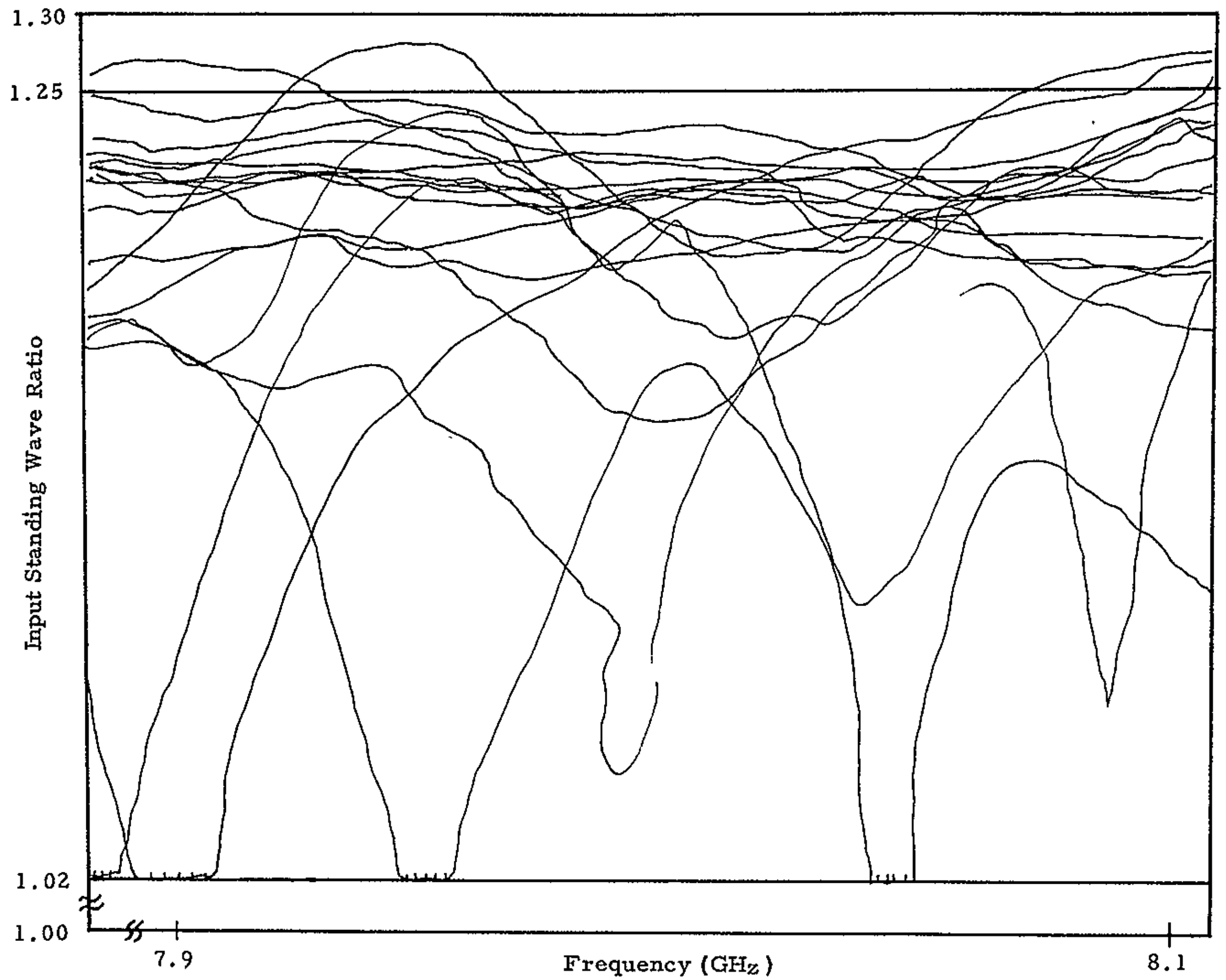

Figure 27. Swept Frequency Plot of Input VSWR for Each of the Inputs to the Switch. (Each measurement was made with the switch set to receive from that port being tested.)

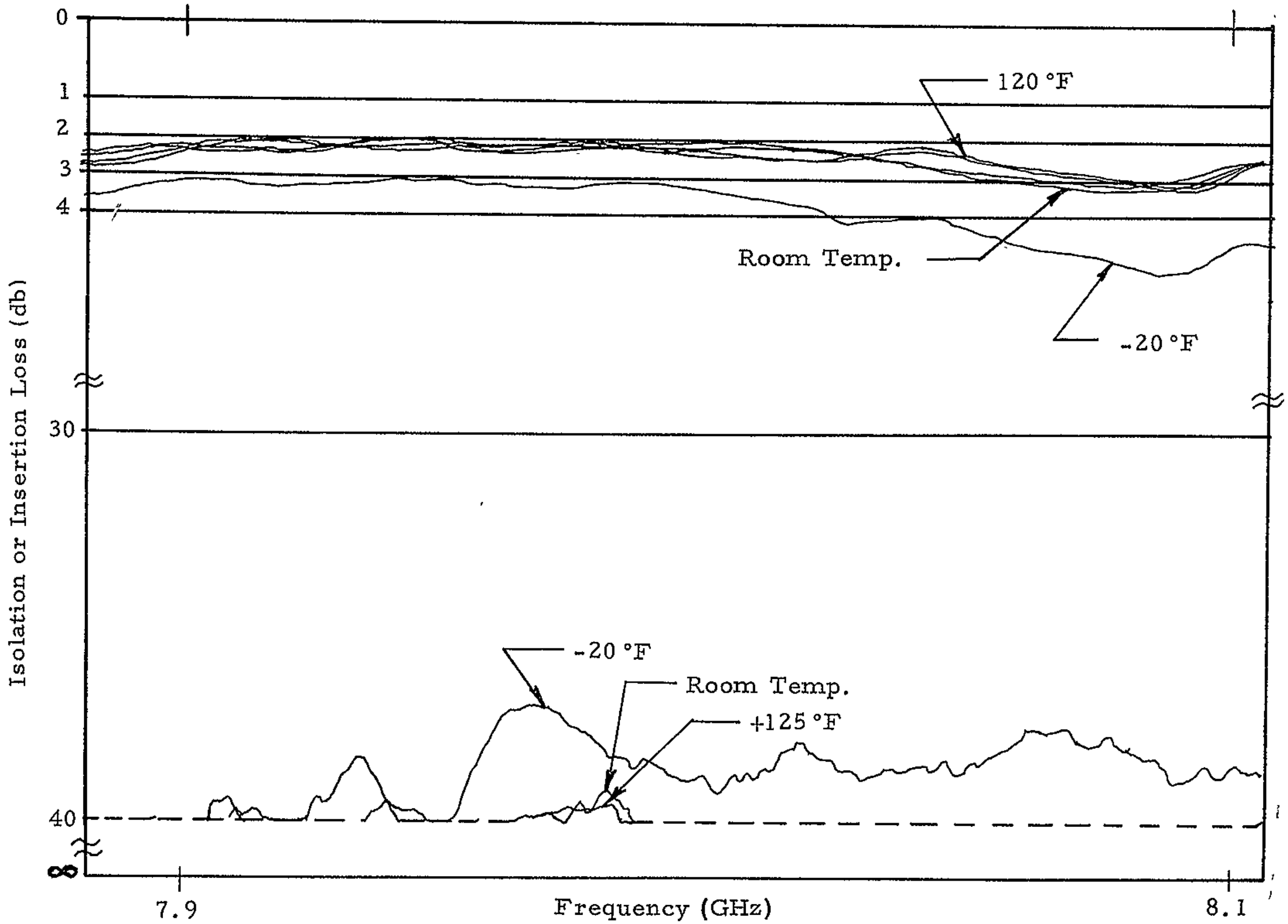

Figure 28. Frequency Variation of Isolation and Insertion Loss with Ambient Temperature as a Parameter. (Insertion loss and isolation measurements were made in a manner similar to that used in obtaining Figure 24, except that the isolation is shown for only one port.)

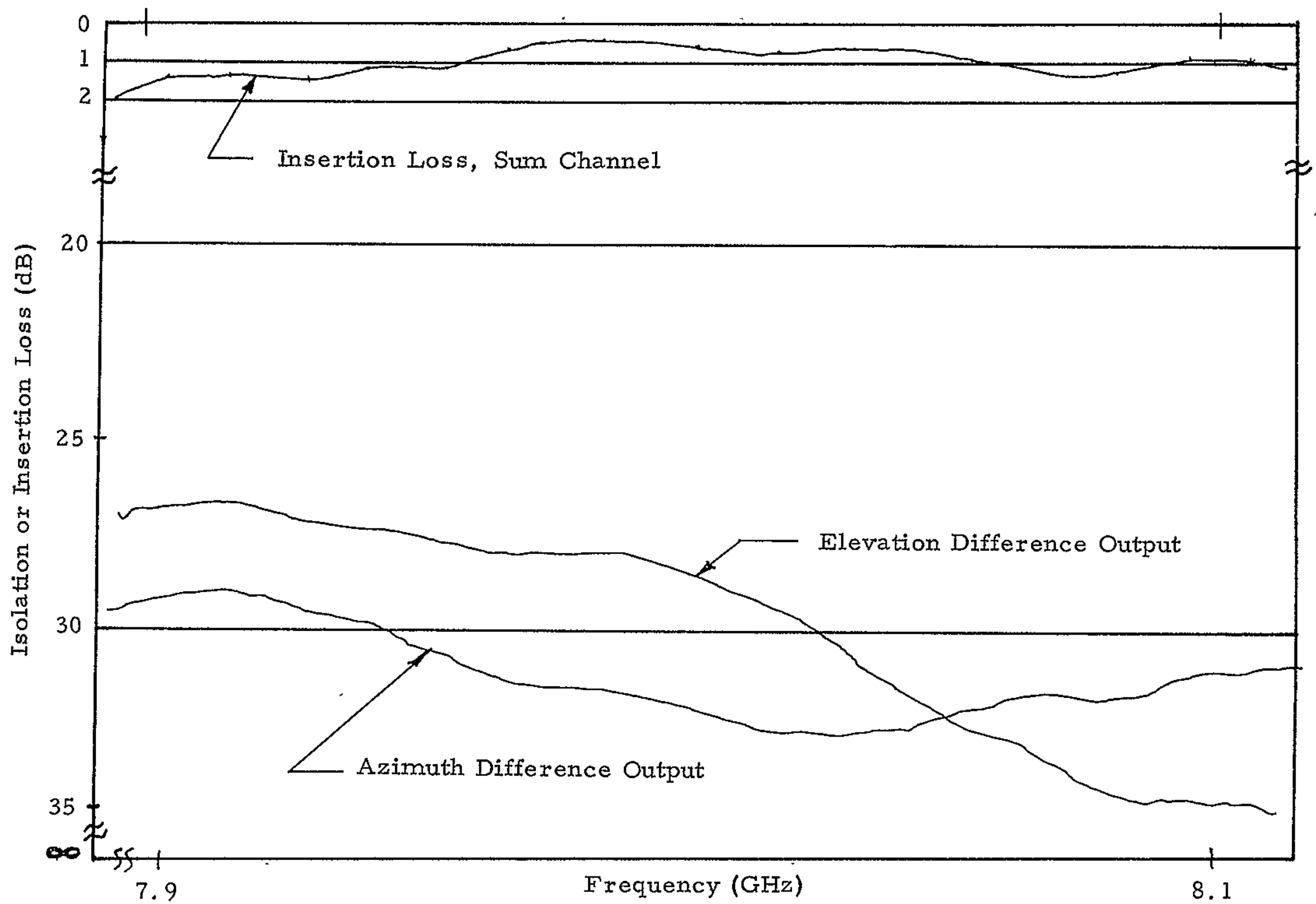

Figure 29. Swept Frequency Plot of Monopulse Converter Characteristics. (In making these measurements 4 signals of equal amplitude and phase were applied to each of the four monopulse inputs (A, B, C and D) as shown in Figure 9.)

4. NEW TECHNOLOGY

The technology used to develop the devices used in the switch reported herein is not considered as new. Considerable work has been carried out previously on Contract DA 28-043-AMC-02445(E), Broadband Latching Switches and Circulators. A full discussion of the construction of latching circulators has been presented in the quarterly reports issued under this contract.

5. BIBLIOGRAPHY

1. J. Simon, et al, "Microwave Ferrite Devices (Octave Bandwidth Y-Junction Circulators)," Final Report, U.S. Army Electronics Laboratories, Fort Monmouth, New Jersey, Contract Number DA36-039SC-89214.

2. H. Bosma, "On the Principle of Stripline Circulation," Proc. of the Institute of Electrical Engineers, Vol. 109, Part B, Supplement No. 21, January 1963, p. 137.

3. H. Bosma, "On Stripline Y-Circulation at HUF," IEEE Trans., Vol. MTT-12, pp. 61-72, January 1964.

4. C. E. Fay and R. L. Comstock, "Operation of the Ferrite Junction Circulator," IEEE Trans., Vol. MTT-13, pp. 15-27, January 1965.

5. R. L. Comstock, and C. E. Fay, "Performance and Ferrimagnetic Material Considerations in Cryogeni Microwave Devices," presented at the Magnetism and Magnetic Materials 10th Conference, 1964.

6. Ernest Stern and William J. Ince, "Design of Composite Magnetic Circuits for Temperature Stabilization of Microwave Ferrite Devices," IEEE Trans. Vol. MTT-15, pp. 295-300, May 1967.

7. Richard W. Peters, et al, Handbook of Tri-Plate Microwave Components, Sanders Associates, Inc., Nashua, New Hampshire, 1956.